

Quark-hadron phase transition in the early Universe: Isothermal baryon-number fluctuations and primordial nucleosynthesis

G. M. Fuller, G. J. Mathews, and C. R. Alcock

*Institute of Geophysics and Planetary Physics, University of California, Lawrence Livermore National Laboratory,
Livermore, California 94550*

(Received 11 September 1987)

We study the quark-hadron transition in the early Universe and compute the amplitude of isothermal baryon-number fluctuations that emerge from this transition along with their effects on a primordial nucleosynthesis. We find that such fluctuations are a natural consequence of a first-order phase transition occurring in the strongly interacting system. Fluctuation-generating mechanisms are discussed. We estimate the nucleation rate and derive the mean separation between fluctuations. It is shown that the amplitude of the fluctuations depends sensitively on the phase coexistence temperature T_c and on the baryon transmission probability Σ_h at the phase boundary. For realistic values of Σ_h and T_c the fluctuations are large and have a significant effect on primordial nucleosynthesis yields. With these fluctuations the limit on the baryonic contribution to Ω depends primarily on what is taken to be the primordial ${}^7\text{Li}$ abundance: $\Omega=1$ in baryons would require large ${}^7\text{Li}$ and ${}^2\text{H}$ destruction factors during the evolution of the Galaxy.

I. INTRODUCTION

A transition from quark-gluon plasma to confined hadronic matter must have occurred at some point in the evolution of the early Universe. There may be a first-order phase transition at this epoch associated with either the color-confinement transition¹ or the chiral-symmetry-breaking transition.² Even a simple model of deconfined quark-gluon plasma with asymptotic freedom shows that if the Universe were ever at a temperature in excess of ~ 100 MeV then a color-deconfined plasma should be the most stable phase. For this reason alone, it is certainly of interest to explore whether there might be a relic signature of the quark-hadron transition in primordial light-element abundances or elsewhere. The purpose of this paper is to address these issues.

There have been several recent papers³⁻⁵ based on the possibility that the quark-hadron phase transition in the early Universe may have led to the formation of isothermal baryon-number fluctuations. The basis for the production of isothermal baryon-number fluctuations from a phase transition in the early Universe lies in the separation of cosmic phases scenario first discussed by Witten⁶ and later by Applegate and Hogan.⁷

The separation of cosmic phases scenario runs as follows. At a high enough temperature in the early Universe ($T > 1$ GeV) the color charges, carried by quarks and gluons, are unconfined, and a plasma of relativistic quarks and gluons obtains. As the Universe expands, the temperature drops through T_c , the coexistence temperature where, in principle, the quark-gluon plasma could exist in pressure and chemical equilibrium with a dense and hot gas of hadronic states (pions, neutrons, protons, deltas, etc.) where color charges are confined. This new phase is not nucleated immediately at T_c , since a generic feature of quantum or thermal nucleation is

that the nucleation rate does not become large until the temperature has dropped below the coexistence temperature.⁸ In other words, supercooling occurs until the probability to nucleate bubbles of hadronic phase is high.

Once the first generation of nucleated bubbles of hadron phase appears, the release of latent heat from the QCD vacuum energy reheats the Universe to T_c , so that further nucleation of hadronic phase is inhibited. The quark-gluon plasma phase and the confined, hadronic phase now coexist in pressure equilibrium. As the Universe expands the temperature is held at T_c by the liberation of latent heat as the confined phase grows at the expense of the unconfined phase. This nearly isothermal evolution may continue until all of the Universe has been converted to confined phase. This scenario has been discussed in some detail by Kajantie and Kurki-Suonio.⁹

We will show that isothermal baryon density fluctuations could arise during this cosmic separation of phases scenario. We will discuss the microphysics of the fluctuation generation mechanisms and we identify two scenarios. In the limit of chemical equilibrium between the two phases in coexistence there will be a different baryon concentration in each phase. In the limit where the exchange of baryon number across the boundary between the two phases is not rapid enough to achieve chemical equilibrium, the fluctuations generated are always larger than in the equilibrium case, since nucleated confined vacuum contains no net initial baryon number.

These scenarios for the generation of fluctuations depend on the phase transition being first order so that latent heat is released. Lattice gauge QCD with dynamical fermions suggests that a phase transition associated with either the quark-hadron transition or the chiral-symmetry transition is at least weakly first order, but this has not yet been conclusively demonstrated.^{2,10-12}

The isothermal density fluctuations from the quark-hadron phase transition could be further modified at a

later epoch by a diffusive separation of neutrons and protons, as pointed out by Applegate, Hogan, and Scherrer,³ resulting in low-density neutron-rich regions and high-density proton-rich regions at the time of nucleosynthesis. The primordial nucleosynthesis resulting from a universe which is inhomogeneous in density and neutron-to-proton ratio is very different from that in the standard big bang and, in fact, may give acceptable light-element abundances even with $\Omega=1$ in baryons. For $\Omega=1$ in baryons, ${}^4\text{He}$, ${}^2\text{H}$, and possibly ${}^3\text{He}$ can be within observational constraints independent of the size of the fluctuations once the fluctuations are sufficiently large. However, ${}^7\text{Li}$ appears to be overproduced in both the neutron- and proton-rich phases. This over production may be acceptable (given the uncertainties of the ${}^7\text{Li}$ abundance) if there has been significant stellar destruction of ${}^7\text{Li}$ and ${}^2\text{H}$.

The fact that primordial nucleosynthesis in this scenario allows for $\Omega=1$ in baryons may resolve the discrepancy between the predictions of inflationary cosmology and standard big-bang nucleosynthesis. The inflationary model of the Universe gives a compelling solution to the horizon and flatness problems in cosmology^{13,14} and predicts that the geometry of the Universe should be flat to high accuracy. In the case of zero cosmological constant, inflation predicts that the ratio of the mass energy density to the closure density, Ω , should be unity.^{13,14} Estimates of the amount of mass energy present in the Universe from observations of luminous matter fall short of closure ($\Omega=1$), yet there are observational indications of nonluminous "dark matter" in galactic halos and clusters of galaxies which may make up the shortfall and produce $\Omega=1$ (Ref. 15) and galaxy number counts now also seem to indicate that $\Omega=1$ (Ref. 16).

It is believed that this dark-matter component cannot be or have been baryonic in nature, because standard big-bang nucleosynthesis with $\Omega=1$ in baryons gives primordial abundances which are inconsistent with observation; in particular, not enough deuterium is produced.^{17,18} It is not known what the dark-matter component is. There are many candidate particles but either they have not been experimentally detected, or their masses have not been unambiguously determined.¹⁹ Standard big-bang nucleosynthesis is not lightly discarded, however, because with a minimum of assumptions it can reproduce observed light-element abundances^{17,18} and put limits on neutrino masses and numbers of lepton generations that are in fair agreement with independent experimental determinations.¹⁹⁻²¹ Nevertheless, the dark-matter component remains unknown and this, in turn, invites speculation.

Our primary objectives in this work are thus to calculate the amplitude of the isothermal baryon-number fluctuations arising from the quark-hadron transition, identify the key pieces of strong-interaction physics which determine this amplitude, estimate the density of nucleation sites, and compute in detail the effect of these isothermal baryon-number fluctuations on primordial nucleosynthesis. We will emphasize that baryon-number fluctuations are a *natural* consequence of a first-order phase transition in the early Universe and require *no*

fine-tuning of parameters. In fact, we will show that these fluctuations arise in a manner akin to the well-known impurity concentrating techniques in metallurgy, such as zone refining of semiconductors. This paper is an extension of our previous work⁵ in that we explore in considerably more detail several possible mechanisms for producing the fluctuations and look at the nucleation process in more depth. We also utilize primordial nucleosynthesis to identify both constraints on the nature of the quark-hadron phase transition from light-element abundances and the conditions necessary for $\Omega=1$ in baryonic matter.

II. THERMODYNAMICS OF THE QUARK-HADRON PHASE TRANSITION

It will be most convenient for our purposes to compute the thermodynamic potential Ω for both the quark-gluon plasma phase and the hadron phase. We caution that we have used the symbol Ω for both the thermodynamic potential and the critical parameter for the Universe. It should be clear from the context which Ω we intend. Our definition of Ω conforms with that in Landau and Lifshitz,²² so that

$$\Omega = -T \ln(Z), \quad (1)$$

where Z is the grand partition function. Ω is a function of temperature (T), chemical potential (μ), and volume (V). In this definition the thermodynamic variables corresponding to Ω are

$$P = - \left[\frac{\partial \Omega}{\partial V} \right]_{T, \mu} = -\Omega/V, \quad (2a)$$

$$n = - \frac{1}{V} \left[\frac{\partial \Omega}{\partial \mu} \right]_{V, T}, \quad (2b)$$

$$S = - \left[\frac{\partial \Omega}{\partial T} \right]_{V, \mu}, \quad (2c)$$

$$E = -PV + ST + \mu nV, \quad (2d)$$

where P , n , S , and E are, respectively, the pressure, particle number density, entropy, and energy.

A first-order phase change occurs when there are two (or more) physically distinct organizations of the statistical degrees of freedom which can occur for the same (T, μ) . The more stable phase has the lower Ω (higher P), and the two phases coexist when $P_q = P_h$ (where q = quark phase, h = hadron phase), which yields a coexistence curve $T = T_c(\mu)$. In the early Universe $\mu \ll T$. The latent heat per unit volume in the phase change is

$$L = T_c \frac{\partial}{\partial T} (P_q - P_h) = T_c (s_q - s_h), \quad (2e)$$

where the derivative is evaluated at constant μ and at $T = T_c$, and s_q and s_h are entropy densities in the quark-gluon and hadron phases, respectively.

The equilibrium baryon-number densities in the two phases are given by (2b). Since the two thermodynamic potentials have very different dependencies on μ , there will be a significant baryon-number density contrast

across the phase boundary. This and other effects will lead to isothermal baryon-number fluctuations.

It is straightforward to compute the grand partition function, and thus Ω , if we assume that the particles are noninteracting except for an overall QCD vacuum energy in the unconfined phase. The background relativistic particles which are not strongly interacting and are in thermal equilibrium with both the confined and unconfined phases contribute (for $\mu=0$)

$$\Omega = -V(g_b + \frac{7}{8}g_f)\frac{\pi^2}{90}T^4, \quad (3a)$$

where g_b and g_f are the statistical weights of bosons and fermions, respectively. At the epoch of the quark-hadron phase transition photons ($g_b=2$), electrons ($g_f=4$), muons ($g_f=4$), and neutrinos ($g_f=6$), yield $g = g_b + \frac{7}{8}g_f = 14.25$ so that the pressure contribution from these particles common to both phases is

$$P \simeq 1.56T^4. \quad (3b)$$

We treat the unconfined quark-gluon plasma as a gas of noninteracting relativistic particles plus an overall vacuum energy. In the limit of vanishing quark masses, there is a simple expression for Ω which is valid for any temperature and chemical potential:²³

$$\Omega_{qg} = \frac{-7\pi^2}{180}N_c N_f VT^4 \left[1 + \frac{30}{7\pi^2} \left(\frac{\mu_q}{T} \right)^2 + \frac{15}{7\pi^4} \left(\frac{\mu_q}{T} \right)^4 \right] - \frac{\pi^2}{45}N_g VT^4 + BV, \quad (4a)$$

$$\Omega_{qg} \simeq -37\frac{\pi^2}{90}VT^4 + BV. \quad (4b)$$

Here N_c is the number of colors (three), N_f is the number of relativistic quark flavors (two at lower temperatures corresponding to the u and d quarks, and three at higher temperatures where the strange quark becomes relativistic), and B is the QCD vacuum energy, or bag constant. The number of gluons is $N_g=8$. The quark chemical potential is $\mu_q = \frac{1}{3}\mu_b$, where μ_b is the baryon chemical potential.

For the early Universe ($\mu_b/T \sim 10^{-8}$), so that for two relativistic quark flavors the contribution to the pressure in the unconfined phase from quarks and gluons is

$$P \approx 4.06T^4 - B. \quad (4c)$$

The total pressure in the early Universe in the unconfined phase includes the contributions from Eqs. (3b) and (4c).

Note that the QCD vacuum energy contributes negatively to the pressure. The value of this vacuum energy, or bag constant, is not known and in what we have done it serves to parametrize the temperature at which the confined and unconfined phases coexist. We emphasize that in what follows it will be this coexistence temperature, T_c , which will be the fundamental quantity of interest. The vacuum-energy (bag-model) approach is simply an easy and concise way to calculate the essential thermodynamics of the unconfined phase in a consistent manner.

We caution that for two reasons it is difficult to connect the value of the bag constant used in various models of hadrons with the relevant value of B in Eqs. (4a) and (4b). First, most current research on modeling hadronic properties with the bag must address the problem of treating the bag surface.²⁴⁻²⁹ Surface effects can be appreciable for individual hadrons. However, as will be shown below, we expect the regions of unconfined quark-gluon plasma which are in coexistence with confined hadronic matter to be of macroscopic size, so that surface effects are minimal. Second, it is dangerous to use a value of B in Eqs. (4a) and (4b) that is derived from a particular model of hadrons because we are interested in the *high-temperature* QCD vacuum energy. This vacuum energy probably comes down with increasing temperature.²⁷ For example, the finite-temperature corrections from gluon exchange can cause the effective value of the QCD vacuum energy to drop.^{25,29}

In short, for our purposes in modeling the bulk thermodynamics of the quark-gluon plasma we must treat the QCD vacuum energy and corresponding coexistence temperature as unknown quantities. The coexistence temperature can be a crucial determinant of the size of isothermal baryon-number fluctuations in the early Universe. We will take a range in B between $(50 \text{ MeV})^4$ and $(300 \text{ MeV})^4$ corresponding to coexistence temperatures between 40 and 250 MeV (cf. Fig. 3 below). This range will include all currently discussed values of the QCD vacuum energy, from the low value of $B = (145 \text{ MeV})^4$ in the MIT bag^{26,27} model to the rather large values, $B = (278 \text{ MeV})^4$, used in most early Universe studies.⁹ Because of the above caveats we put no stock in any of these values for B as such, and emphasize that only the coexistence temperature is fundamental to our analysis.

For the confined, or hadronic, phase we will not use the bag model but rather the spectrum³⁰ of known masses for baryons and mesons. This is not inconsistent with the bag-model treatment of the quark-gluon phase because the isothermal baryon-number fluctuations we are interested in are largest at low coexistence temperature where the neutron, proton, pion, and other light hadron masses (which do not depend on B) dominate the hadronic level density. At higher temperatures there may be an inconsistency and we discuss this limit below.

Computing Ω for mesons first (note that $\mu=0$ for the mesons), we find for each meson that

$$\Omega = \frac{-gVT^4}{\pi^2} \sum_{n=1}^{\infty} \frac{1}{n^4} \bar{K}_2(nm/T), \quad (5a)$$

where m is the mass of the meson, and g is the spin plus isospin degeneracy factor, $g = (2J+1)(2I+1)$. The \bar{K}_2 is related to the modified Bessel function of the second order (K_2), as in Fowler and Hoyle,³¹

$$\bar{K}_2(x) \equiv \frac{x^2}{2} K_2(x). \quad (5b)$$

Note that

$$\lim_{x \rightarrow 0} \bar{K}_2(x) = 1, \quad (5c)$$

and for $x \gg 1$,

$$\bar{K}_2(x) \approx \left[\frac{\pi x^3}{8} \right]^{1/2} e^{-x} \left[1 + \frac{15}{8x} + \frac{105}{128x^2} + \dots \right]. \quad (5d)$$

In the high-temperature limit ($T \gg m$),

$$\Omega = -\frac{\pi^2}{90} g V T^4. \quad (5e)$$

In the conditions we are interested in ($T \sim 100$ – 200 MeV) the pions will make the dominant contribution to the pressure in the hadronic phase, so that Eq. (5e) with $g = 3$ yields a useful approximation to the thermodynamic potential for the hadrons. However, in the numerical calculations presented below we have summed the contributions to Ω in Eq. (5a) over all of the known mesons and calculated all \bar{K}_2 numerically. Masses, spins, and isospins of these particles are taken from the Particle Data Group summary.³⁰

For baryons in the small chemical potential limit ($|\mu_b| < m$),

$$\Omega = \frac{-2gT^4V}{\pi^2} \sum_{n=1}^{\infty} \frac{(-1)^{n+1}}{n^4} \cosh \left[\frac{n\mu_b}{T} \right] \bar{K}_2(nm/T). \quad (6a)$$

The net baryon-number density corresponding to this Ω is

$$n_b = \frac{2gT^3}{\pi^2} \sum_{n=1}^{\infty} \frac{(-1)^{n+1}}{n^3} \sinh \left[\frac{n\mu_b}{T} \right] \bar{K}_2(nm/T). \quad (6b)$$

Note that n_b is the number density of baryons minus that of the antibaryons. As above, we obtain the total Ω by summing over the spectrum of known baryonic masses.³⁰

It is possible to make a simple analytic model of the essential statistical mechanics of the quark-hadron system and compare this to our numerical results. We define $a \equiv \pi^2/30$ and the statistical weight for the photons, neutrinos, electrons, and muons common to both phases as $g_{\nu\gamma} = 14.25$. We then define the intrinsic statistical weight for the quark-gluon plasma as g_Q and that for the hadron soup as g_H . The total statistical weight for each phase in coexistence is then defined as

$$g_q \equiv g_Q + g_{\nu\gamma}, \quad (7a)$$

$$g_h \equiv g_H + g_{\nu\gamma}. \quad (7b)$$

In the model of the quark-gluon plasma discussed above $g_Q = 37$ and thus $g_q \approx 51.25$. At $T_c \sim 100$ MeV the pions dominate the contribution to Ω in the sum of Eqs. (5a) and (6a), so that very roughly $g_H \approx 3$ and $g_h \approx 17.25$. The essential thermodynamics is contained in this difference in statistical weight between the phases.

From Eqs. (2a)–(6a) the pressure P_q , energy density E_q , and entropy density s_q , in the quark-gluon phase are given as

$$P_q = \frac{1}{3} g_q a T^4 - B, \quad (8a)$$

$$E_q = g_q a T^4 + B, \quad (8b)$$

$$s_q = \frac{4}{3} g_q a T^3, \quad (8c)$$

while for the hadron phase the corresponding quantities are

$$P_h = \frac{1}{3} g_h a T^4, \quad (9a)$$

$$E_h = g_h a T^4, \quad (9b)$$

$$s_h = \frac{4}{3} g_h a T^3. \quad (9c)$$

We define the ratio of statistical weights in the two phases to be

$$x = \frac{g_q}{g_h} = \frac{s_q}{s_h} \rightarrow 2.971 \text{ at } T_c \sim 100 \text{ MeV}. \quad (10)$$

Note that x in this paper is the same as r in Ref. 9. Inclusion of the hadronic resonances makes g_h , and hence x , a function of temperature. Likewise, since the number densities of hadrons are large at high temperature [Eqs. (5a)–(6a)] interaction corrections to g_h and x may be appreciable. In Fig. 1 we present x as a function of temperature for the known mass spectrum of hadrons³⁰ and different numbers of relativistic quark flavors. At lower temperature, when baryon-number fluctuations are expected to be largest, temperature and interaction corrections to x will be small.

The latent heat given in Eq. (2e) can be expressed as

$$L = T_c s_q \left[1 - \frac{1}{x} \right] \approx 4B, \quad (11)$$

where the latter approximation follows for constant $x = 2.971$. Figure 2 gives the latent heat as a function of temperature. Note the rapid change in L at high temperature, $T \geq 200$ MeV due to the increased pressure from higher-lying hadronic resonances.

Pressure equilibrium, or coexistence, between the phases $P_h = P_q$, occurs for a temperature

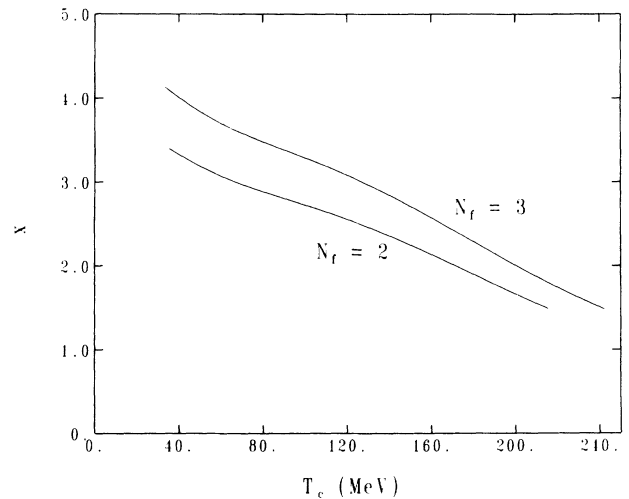


FIG. 1. The ratio of the effective statistical weights of the unconfined phase to the confined phase x as a function of coexistence temperature T_c . The contribution of all known hadronic resonances is included in the computation of the pressure equilibrium.

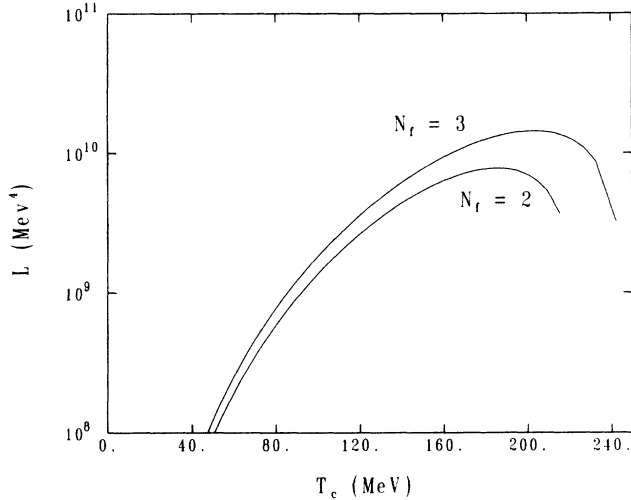


FIG. 2. The latent heat L as a function of coexistence temperature T_c . This calculation includes a sum over all hadronic resonances.

$$T_c = (g_q - g_h)^{-1/4} \left[\frac{3}{a} \right]^{1/4} B^{1/4} \approx 0.72 B^{1/4}, \quad (12)$$

where the latter approximation assumes $x = 2.971$. Figure 3 gives a plot of $B^{1/4}$ vs T_c obtained by including the sum over hadronic resonances in the computation of pressure equilibrium. Values of $B < (300 \text{ MeV})^4$ lead to a coexistence temperature $T_c < 250 \text{ MeV}$, in which the separation of phases scenario outlined above could produce isothermal baryon-number fluctuations of appreciable amplitude. If the QCD vacuum energy is $B > (300 \text{ MeV})^4$, then no coexistence of phases would be possible in the simple model presented here. However, hadronic interactions should lead to a phase transition at some point, but this case is not interesting to us because the coex-

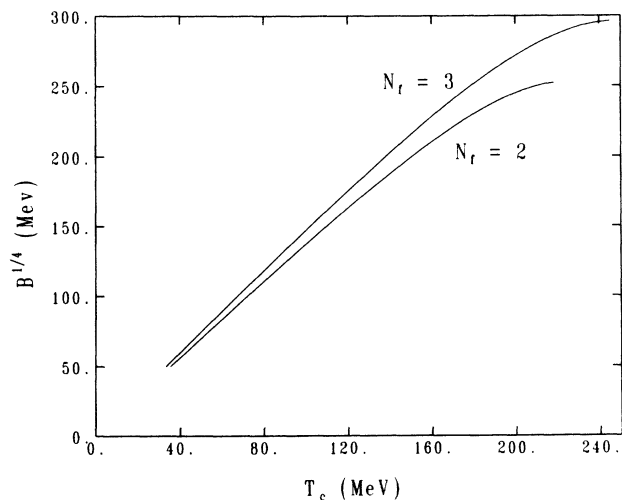


FIG. 3. The QCD vacuum energy $B^{1/4}$ as a function of coexistence temperature T_c for two and three relativistic quark flavors.

istence temperature is too high for fluctuations to have an appreciable amplitude.

Finally, even if the QCD vacuum energy is high, $B \sim 300 \text{ MeV}$, it might be possible that the quark-gluon plasma phase is able to supercool well below T_c before nucleation of the hadronic phase begins. In this extreme case the QCD vacuum energy will come to dominate the pressure of the Universe and a short de Sitter exponential expansion of the Universe can ensue. This mini-inflation, however, could result in only a 15% increase in the scale factor.⁵

III. NUCLEATION

When a thermodynamic system is cooled (or heated) through the coexistence temperature at which a first-order phase transition occurs, the new phase does not appear immediately. Significant reorganization of fundamental degrees of freedom is needed for the creation of the new phase, and the thermodynamic fluctuations which can produce such reorganization have low probability. Furthermore, it is energetically unfavorable to create small volumes of new phase because of the free energy associated with the surface separating the two phases. These effects ensure that some supercooling below the coexistence temperature occurs before stable nuclei of the new phase are produced. These nuclei grow rapidly, since the old phase is metastable, releasing latent heat and thus reheating the system back to the coexistence temperature.

The physics of nucleation in the quark-hadron phase transition is even less well understood than the bulk thermodynamics. However, there are three plausible mechanisms for this process. We call these mechanisms homogeneous nucleation, heterogeneous isothermal nucleation, and heterogeneous nonisothermal nucleation.

A. Homogeneous nucleation

If the Universe is *pure* and *isothermal*, then the new phase originates through spontaneous fluctuations in the metastable phase, a process known as homogeneous nucleation.²² We will quantify the meanings of “pure” and “isothermal” in Secs. III B and III C, respectively.

The nucleation rate is determined by the probability that a spontaneous fluctuation in the metastable (quark) phase will produce a “critical nucleus” of the stable (hadron) phase. This critical nucleus has a radius r_c determined by

$$P_h - P_q = \frac{2\sigma}{r_c}, \quad (13)$$

where σ is the free energy per unit surface area associated with the boundary of the nucleus, which is assumed to be spherical.

New nuclei with radii less than r_c will collapse and disappear, while nuclei of radii larger than r_c will expand until a macroscopic amount of new phase is produced. The probability of a fluctuation of radius r_c is $\exp(-W/T)$ where

$$W = \frac{4\pi}{3} r_c^3 (P_q - P_h) + 4\pi\sigma r_c^2. \quad (14)$$

The first term in (14) is the difference between the thermodynamic potentials of the two phases and is negative. The second term is the surface free energy of the boundary between the phases.

The rate $p(T)$ at which nuclei form per unit volume per unit time is given by²²

$$p(T) = CT_c^4 \exp(-W/T), \quad (15)$$

where C is a coefficient of order unity, which turns out (see below) to have no quantitative significance when we calculate the number density of nucleation sites. Note that if the nucleation rate were extremely fast, then the number of nucleated bubbles would be so large that it would look like the vacuum changed phase around the quarks and gluons present. We now argue that the nucleation rate is probably not this fast.

It will turn out that the amount of supercooling is very small. Accordingly, it is convenient to expand about the coexistence temperature T_c . From Eq. (2e) we define

$$P_h - P_q = L\eta, \quad (16a)$$

$$\eta \equiv \frac{T_c - T}{T_c}, \quad (16b)$$

where L is the latent heat per unit volume of the phase transition and η is the "supercooling parameter." It follows that

$$p(\eta) \approx CT_c^4 \exp\left[-\frac{16\pi}{3} \frac{\sigma^3}{T_c L^2 \eta^2}\right]. \quad (17)$$

The important characteristics of Eq. (17) are that $p(T) \rightarrow 0$ as $T \rightarrow T_c$, and that for small supercooling ($\eta \ll 1$) the argument of the exponential is large and negative, yielding a very strong increase of p with η . This means that almost all nucleation occurs at the lowest temperature achieved during the supercooling phase (i.e., just prior to reheating). Furthermore, metastable regions are reheated by the release of latent heat around individual nucleation sites, and no appreciable nucleation occurs in the reheated regions.

The important parameter for the purpose of primordial nucleosynthesis will be the mean comoving distance between nucleation sites. We estimate this distance from Eq. (17) for a given nucleation rate, using an analysis similar to that of Kajantie and Kurki-Suonio.⁹ In this analysis, each expanding volume of hadronic phase acts as a piston driving a weak shock wave which expands into the quark phase at just above the sound speed $V_s \approx 3^{-1/2}$. These shocks reheat the quark material. No further nucleation will occur once a region has been crossed by one or more shocks. Then it follows that the fraction of the Universe which is unaffected by nucleation during this period is

$$f(t) = \exp\left[-\int_{t_c}^t f(t') p(T') dt' \frac{4\pi}{3} V_s^3 \left(\frac{T}{T'}\right)^3 \times (t-t')^3\right]. \quad (18)$$

The total number density of nucleation sites is

$$N_n = \int_{t_c}^{\infty} f(t) p(T) dt. \quad (19)$$

In these equations t is time, t_c is the time at which the Universe first cools through $T = T_c$, T is the temperature at time t , and T' the temperature at time t' . The solution of Einstein's relativistic field equation yields a relation between the age of Universe, t , and the temperature,

$$t = \left[\frac{9}{164\pi^3 G}\right]^{1/2} \frac{1}{T^2}, \quad (20)$$

where G is Newton's constant, and the energy density due to the quarks has been included.

Given the very rapid rise of nucleation rate p with time, a reasonable approximation to Eq. (18) is

$$f(t) \approx \begin{cases} 1 - \int_{t_c}^t dt' p(T') \frac{4\pi}{3} V_s^3 (t-t')^3, & t < t_f, \\ 0, & t \geq t_f, \end{cases} \quad (21)$$

where t_f is the time when the entire Universe has been reheated. Note that $f(t)$ resembles a step function so that we can approximate Eq. (19) as

$$N_n \approx \int_{t_c}^{t_f} p(t) dt, \quad (22)$$

where we have written the nucleation rate as a function of time using Eq. (20).

Further progress in determining the extent of supercooling may be made by expanding about $t = t_f$, or $T = T_f$, as

$$\ln p(T) = \ln p(T_f) + \left[\frac{d \ln p}{dT}\right]_{T_f} \left[\frac{dT}{dt}\right]_{t_f} (t - t_f), \quad (23a)$$

i.e.,

$$p(t) = p(t_f) \exp[-\alpha(t_f - t)], \quad (23b)$$

where p is now expressed as an explicit function of time, and

$$\alpha = \frac{32\pi^2}{9} (41\pi G)^{1/2} \frac{\sigma^3 T_c^4}{L^2 (T_c - T_f)^3}. \quad (24)$$

The expansions (23) and (24) may be used in (21) to evaluate the integral and to find t_f , T_f , and η_f with the result

$$\eta_f^{-12} \exp\left[\frac{16\pi}{3} \frac{\sigma^3}{T_c L^2 \eta_f^2}\right] = \frac{3^8}{2^{12} 41^2 \pi^9} \frac{CL^8 V_s^3}{\sigma^{12} G^2}. \quad (25)$$

An approximate solution of (25) is

$$\eta_f \approx 1.4 \frac{\sigma^{3/2}}{T_c^{1/2} L}, \quad (26)$$

when σ is near its upper limit.

The right-hand side of Eq. (25) is very large because G is very small. This ensures that η_f is small; the degree of supercooling is small because the Universe expands very slowly compared to the natural time scales in QCD. The degree of supercooling is determined by σ , L , T_c , and G and depends only weakly on C .

It is also possible to evaluate the number density of nucleation sites given by Eq. (22) using Eqs. (20) and (22)–(24), with the result

$$N_n t^3 = \pi^2 \left[\frac{8}{3} \frac{\sigma^3}{V_s T_c L^2 \eta_f^3} \right]^3. \quad (27)$$

An important quantity for nucleosynthesis is the mean separation l per nucleation site. Combining Eqs. (27) and (26) yields

$$l \equiv N_n^{-1/3} \approx 0.3 \frac{\sigma^{3/2} t}{T_c^{1/2} L}, \quad (28a)$$

$$l \approx (5.43 \times 10^6 m) \frac{\sigma^{3/2}}{T_c^{13/2}} \\ \approx (2 \times 10^6 m) (\sigma / \text{MeV}^3)^{3/2} (T_c / \text{MeV})^{-13/2}, \quad (28b)$$

where the second equation follows from the thermodynamic model of the preceding section. This length scale should be greater than the comoving proton diffusion length in order that the fluctuations not damp out entirely before the onset of nucleosynthesis (see the discussion in Sec. VII below). In addition, should this length turn out to be greater than the comoving neutron diffusion length, then the approximate treatment of diffusion and nucleosynthesis that is described in Sec. VII is inadequate; however, there will still be significant modification of the nucleosynthesis yield and our broad conclusion will be qualitatively correct.

This length scale depends on two bulk properties of the phase transition (T_c and L) that may be calculated in terms of our model equations. In addition, this length scale depends on the surface tension σ for which we have no model calculation. Following Farhi and Jaffe³² and Alcock and Farhi,³³ we expect the “intrinsic” contribution to σ to be small (i.e., $\sigma_I^{1/3} \ll B^{1/4}$) and the “dynamical” contribution to σ to be $\sigma_D \leq (70 \text{ MeV})^3$. If σ is near this upper limit, the length scale (see Table I) is comparable to the comoving neutron diffusion length, which is $\sim 30 \text{ m}$ (Ref. 3).

More important for our analysis would be a lower bound to σ since this would establish whether or not proton diffusion is important. The only strict lower bound is $\sigma > 0$, since $\sigma \leq 0$ would not result in separated phases. It is unlikely that σ is very small compared to the relative contributions of the bulk free energies of the phases, but this possibility cannot be excluded. A characteristic set of possibilities is shown in Table I. Note that the smallest values of l are shorter than the comoving proton diffusion length, which is $\sim 0.5 \text{ m}$ (Ref. 3).

TABLE I. The average distance per nucleation site l is presented for values of the coexistence temperature T_c , the latent heat L , and the surface free energy parameter σ .

T_c (MeV)	L (MeV ⁴)	σ (MeV ³)	l (m)
100	1.5×10^9	3.0×10^5	30
		1.0×10^5	6
		2.5×10^4	0.7
		8.0×10^3	0.1
150	7.0×10^9	3.0×10^5	2
		1.0×10^5	0.4
		2.5×10^4	0.05
		8.0×10^3	0.009

B. Heterogeneous isothermal nucleation

The analysis of homogeneous nucleation assumes that spontaneous fluctuations in the pure metastable phase lead to the appearance of the stable phase. This is rarely the mechanism by which new phases appear in everyday experience or in the laboratory. The appearance of new phases is usually facilitated by impurities (such as dust motes) and by container walls, which serve to reduce the amount of surface free energy needed to produce critical nuclei, or by disturbances (such as cosmic-ray trails in cloud chambers) which produce suprathreshold fluctuations. These processes may be called heterogeneous isothermal nucleation.

At the very high temperatures under discussion there are few candidates for the impurities needed for the heterogeneous nucleation. There may be relic adiabatic fluctuations from the electroweak or other phase transitions, though whether such relics would enhance nucleation in the quark-hadron phases transition is unclear. Most theories indicate that such fluctuations are small on the scale of the particle horizon at the quark-hadron phase transition. More promising in this regard are the various forms of topological singularity: e.g., magnetic monopoles, black holes, and cosmic strings.

Two requirements must be met in order for heterogeneous isothermal nucleation to be important. First, there must be some plausible mechanism by which the nucleation is facilitated. This requirement is probably satisfied by all three candidates. These relic impurities will drive turbulent sound waves into the medium in their vicinity. Temperature fluctuations of amplitude $|\Delta T|/T \geq \eta_f$ will cause a new phase preferentially to appear near these impurities.

The second requirement is that there be enough impurities that heterogeneous nucleation produces more sites than homogeneous nucleation. For the pointlike objects (monopoles, black holes) this means that the number density of impurities must exceed N_n [cf. Eq. (27)]. This is not expected to be the case for either monopoles or black holes.³⁴

However, in some of the models³⁵ of cosmic-string networks, there may indeed be enough loops of string to initiate a significant amount of heterogeneous nucleation. It is easy to show, in these models, that the smallest loops dominate the nucleation. The mean separation between

these loops is $(G\mu)^{1/2}t$ where μ is the mass per unit length, and $G\mu$ is thought to be in the range $10^{-5}-10^{-6}$. Thus, depending on the magnitude of σ , cosmic strings might be the primary agents of nucleation. The scale length, even in this circumstance, is comfortably large compared to the proton diffusion length, so that the fluctuations will persist until the epoch of nucleosynthesis.

C. Heterogeneous nonisothermal nucleation

Should there be significant nonisothermal perturbations at this epoch with $|\Delta T| > \eta_F T_c$, then the spatial scale of nucleation could be set by the spatial scale of these perturbations. We do not, however, have an *ab initio* theory for the generation of such fluctuations.

IV. DYNAMICS OF THE UNIVERSE DURING THE CONSTANT-TEMPERATURE COEXISTENCE EPOCH

The preceding section described the supercooling/nucleation scenario in which the quark-gluon plasma phase is separated from the hadron phase. The duration of this nucleation epoch is short compared to the Hubble time since the fractional supercooling is small ($\eta \sim 10^{-3}$). Again, because the duration of this epoch is short, the entropy generation associated with reheating to T_c is expected to be small compared to the initial entropy. At the end of this nucleation epoch the Universe is left with bubbles of hadron phase surrounded by quark-gluon plasma, all in pressure equilibrium at T_c . Since the hadron bubbles were nucleated through random thermal or quantum processes they contain, on average, no net baryon number; all of the net baryon number resides in the quark-gluon plasma phase.

The subsequent evolution of this configuration of phases takes place at constant temperature T_c (Refs. 6-9). The hadron bubbles grow with time and the fraction of the total volume of the Universe which is in quark-gluon plasma, f_v , decreases from $f_v = 1.0$ to 0 at the end of the phase transition. The Universe remains at constant temperature by trading volume from the unconfined vacuum to the confined vacuum, and thus releasing the latent heat L , depicted in Fig. 2. The detailed dynamics of this constant- T_c epoch have been discussed by Kajantie and Kurki-Suonio.⁹ We summarize the dynamics and specialize our discussion to baryon-number transport in what follows.

If we denote the scale factor in the Robertson-Walker metric by A , then the Einstein equation gives

$$\begin{aligned} \frac{\dot{A}}{A} &= \chi \left[\frac{E_h(1-f_v) + E_q f_v}{B} \right]^{1/2} \\ &= \chi \left[4f_v + \frac{3}{x-1} \right]^{1/2}, \end{aligned} \quad (29)$$

where A is the time derivative of A , f_v is the fraction of the volume of the Universe which is in the quark-gluon plasma phase, and where we have followed Ref. 9 and defined a characteristic QCD expansion rate:

$$\chi \equiv \left[\frac{8\pi G B}{3} \right]^{1/2} \simeq (143 \mu\text{s})^{-1} \left[\frac{T_c}{100 \text{ MeV}} \right]^2. \quad (30)$$

Energy-momentum conservation gives another constraint on the expanding Universe:

$$\dot{P} A^3 = \frac{d}{dt} [A^3(E+P)], \quad (31a)$$

where \dot{P} is the time derivative of the total pressure. To very good approximation $\dot{P} = 0$ during the constant- T_c epoch we consider here, so that the total entropy is constant:

$$\frac{d}{dt} \{ A^3 [f_v s_q + (1-f_v) s_h] \} = 0. \quad (31b)$$

Equation (31b) gives another expression for the expansion rate:

$$\frac{\dot{A}}{A} = \frac{-\dot{f}_v(x-1)}{3f_v(x-1)+3}, \quad (31c)$$

where \dot{f}_v is the fractional rate at which the volume of the Universe is changed from the unconfined to the confined vacuum and is clearly negative.

Equations (29) and (31c) can be solved to yield

$$\begin{aligned} \frac{A(t)}{A_i} &= (4x)^{1/3} \left[\cos \left[\frac{3\chi(t-t_i)}{2(x-1)^{1/2}} \right. \right. \\ &\quad \left. \left. + \arccos \frac{1}{2x^{1/2}} \right] \right]^{2/3}, \end{aligned} \quad (32a)$$

where the beginning of the constant-temperature epoch (end of the nucleation epoch) is taken at time t_i , corresponding to a scale factor $A(t_i) = A_i$. This agrees with Eq. (3.9) in Ref. 9, despite the use of cosines and arccosines here. Similarly it can be shown that

$$\begin{aligned} f_v &= \frac{1}{4(x-1)} \left[\tan^2 \left[\arctan(4x-1)^{1/2} \right. \right. \\ &\quad \left. \left. + \frac{3\chi(t_i-t)}{2(x-1)^{1/2}} \right] - 3 \right], \end{aligned} \quad (32b)$$

where we have assumed that $f_v \approx 1$ at the end of the nucleation phase. This approximation will be adequate for our purpose of following the baryon-number transport properties. Figure 4 shows f_v as a function of time during the constant-temperature coexistence epoch for several values of T_c .

Finally we note that on the completion of the phase transition, where $f_v = 0$, the constant-temperature epoch lasts for a period of time $t_f - t_i \sim$ Hubble time and the ratio of the scale factors is

$$\frac{A_f}{A_i} \approx (x)^{1/3}, \quad (32c)$$

which could have been derived directly by the entropy-conservation condition in Eq. (31b). Note that for $x = 2.971$ the scale factor increases by about 40% during the constant-temperature epoch.

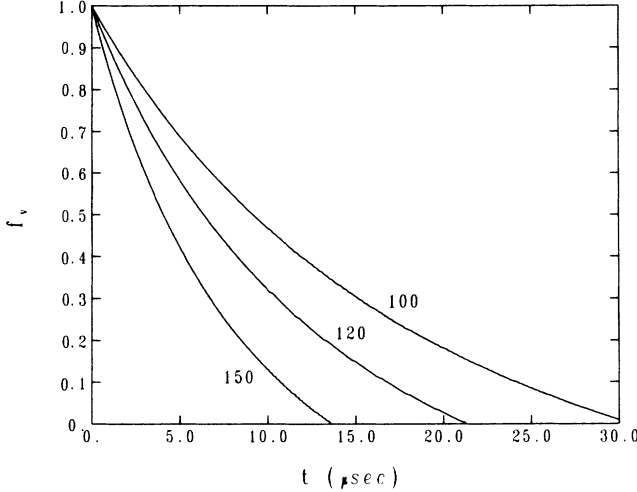


FIG. 4. The quark-gluon plasma volume fraction f_v as a function of the time since the end of the nucleation epoch. Curves for three different values of coexistence temperature, $T_c = 100, 150,$ and 200 MeV are shown.

The total proper surface area Ξ of the boundary which separates the confined and unconfined phases is

$$\Xi \approx 4\pi r^2 N_n V_0, \quad (33a)$$

where N_n ($\sim 10^{-9} \text{ cm}^{-3}$) is the number of nucleated sites per unit volume from Eq. (27), V_0 is the proper volume of the Universe (horizon volume) at the end of the nucleation epoch, and r is taken to be a typical radius of a hadron bubble. Since we have approximated $f_v = 1$ at the beginning of the constant-temperature epoch we must take $r = 0$. As f_v drops from 1.0 to 0.5 the radius of a typical hadron bubble increases from 0 to some maximum value r_{max} . At this point, $f_v = 0.5$, the bubbles of hadron phase percolate with the quark-gluon plasma (turn "inside out"). As f_v drops from 0.5 to 0 we interpret r as the radius of a shrinking bubble of quark-gluon plasma. The assumption of spherical bubbles is strictly correct only near the beginning and the end of the phase transition where the bubble surface energy dominates the volume energy. Nevertheless, the typical bubble radius remains a useful parametrization of the total surface area in the boundary separating the phases, even if the actual surface area is larger than that given in Eq. (33a) because of bubble nonsphericity. During the phase transition the proper bubble radius is

$$r(t) \approx \left(\frac{4}{3}\pi N_n\right)^{-1/3} \frac{A(t)}{A_i} \tilde{f}_v^{1/3}, \quad (33b)$$

where \tilde{f}_v is defined by

$$\tilde{f}_v = \begin{cases} 1 - f_v & \text{if } f_v \geq 0.5, \\ f_v & \text{if } f_v \leq 0.5. \end{cases} \quad (33c)$$

Figure 5 shows the relation between f_v and r for the constant-temperature epoch. The average bubble radius as a function of time $r(t)$ can be found by substituting Eqs. (32a) and (32b) in Eqs. (33b) and (33c).

The approximations presented above for the solution of

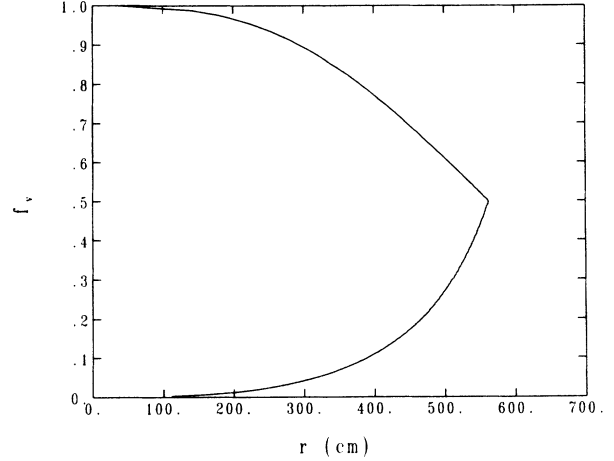


FIG. 5. The quark-gluon plasma volume fraction f_v is plotted against proper bubble radius r . The parameter is interpreted as the radius of a growing bubble of hadron phase for $f_v > 0.5$ and the radius of a shrinking bubble of quark-gluon plasma for $f_v \leq 0.5$.

the phases during the constant-temperature epoch are, at best, a rough approximation but they provide an adequate framework in which to discuss baryon-number transport. Note that, strictly speaking, the entropy cannot remain absolutely constant through the phase transition since a small temperature difference between the phases is required to drive the phase boundary from the hadron phase toward the quark-gluon phase. Solving the hydrodynamic equations for this front results in the phase boundary becoming a condensation discontinuity.²² Such solutions require a very small temperature difference between the phases and, thus, would yield a small entropy generation during the transition.^{6,9}

The constancy of comoving entropy density represented in Eq. (31b) implies that there will be an entropy flux from the quark-gluon plasma phase to the hadron phase as f_v decreases in the constant-temperature epoch. The hydrodynamic models envision this entropy (or enthalpy) flux as being carried by bulk hydrodynamic flow or by neutrinos.⁶⁻⁹ We note that the latent heat associated with the transition is due to converting *volume* from the unconfined to the confined phase. These different vacuum states have different *vacuum energies* and the lower vacuum energy in the confined phase results in increased thermal energy through the creation of particles and particle-antiparticle pairs. The mechanism of heat transport itself will be discussed briefly below as regards fluctuation size. We note however, that hydrodynamic heat transport is favored when the supercooling is small.⁷

The neutrino mean free path is of the order ~ 1 m, so that a neutrino can random walk ~ 1 km, or 10% of the horizon distance, in a Hubble time. On the other hand, the nucleon mean free path is $\sim 10^{-11}$ cm [where the density of mesonic and baryonic states has been estimated using Eqs. (5a)–(6a)] so that a nucleon moves only $\sim 10^{-3}$ cm in a Hubble time. In the simple model of noninteracting quarks and gluons presented here we ex-

pect the quark mean free path to be long compared to the baryon mean free path in the hadron gas.

V. BARYON-NUMBER TRANSPORT ACROSS THE PHASE BOUNDARY AND CHEMICAL EQUILIBRIUM

In this section we will consider the transport of baryon number across the boundary which separates the unconfined and confined phases. We will consider the approach to baryon chemical equilibrium in which the baryon chemical potential μ_b is the same in each phase. The preceding section gave a simple model for the constant coexistence temperature epoch, wherein the evolution of a typical bubble of hadrons or quark-gluon plasma was described. Initially all of the baryon number resides in the quark-gluon plasma and in this section we isolate key features of the physics at the phase boundary which will allow an estimate of the rate at which baryon number leaks from the unconfined phase to the confined phase.

The coexistence of the two phases across a boundary is shown schematically in Fig. 6. Note that the latent heat transport is by the motion of the boundary wall, converting volume from one vacuum to another. This vacuum energy difference can drive particle creation. Neutrinos or photons could carry heat or entropy across the phase boundary, but baryon number is not thermally created in the hadron phase, and thus must actually flow across the boundary if the hadron phase is to have any net baryon number at all. Any transport of baryon number across the phase boundary must be due to strong-interaction processes. We therefore consider two limits to the efficiency of baryon-number transport; The first is that the baryon number is rapidly and efficiently transported across the front to achieve chemical equilibrium; and the second involves an inefficient transport process in which chemical equilibrium is not necessarily achieved on the

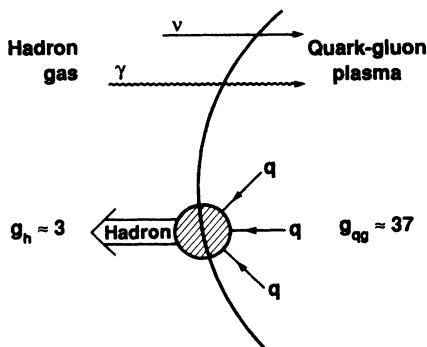


FIG. 6. A schematic illustration of a phase boundary separating the confined vacuum on the left from the unconfined vacuum on the right. The approximate intrinsic statistical weight of relativistic degrees of freedom is shown for each phase. Entropy can be readily carried across the wall by photons, neutrinos, and other light leptons. Baryon number is transported across the boundary only by strong-interaction processes. The indicated processes are reversible.

time scale of the phase-coexistence evolution. We will show that in both of these limits isothermal baryon-number fluctuations will result. It must be emphasized that fluctuations in the distribution impurities are a natural consequence of first-order phase transitions in nature and are exploited in such industrial processes as zone refining of metals and semiconductors. The discussion of the microphysics of the quark-hadron transition to follow serves to illustrate how this transition can behave in a manner akin to the familiar impurity distilling phase transitions despite its exotic setting.

In the limit of chemical equilibrium across the front, the baryon chemical potentials μ_b are equal for the quark-gluon plasma and the hadron gas. Taking the small ($\mu_b/T \approx 10^{-8}$) limit of the expression for the net baryon-number density of the hadron phase in Eq. (6b) we find

$$n_b^h \approx \left[\frac{8}{\pi^3} \right]^{1/2} T^3 \left[\frac{\mu_b}{T} \right] \left[\frac{m}{T} \right]^{3/2} e^{-m/T}, \quad (34)$$

where m is the baryon mass. Note that for a quark-gluon plasma with the same temperature and baryon chemical potential μ_b , the net baryon-number concentration is, from Eqs. (2b) and (4a),

$$n_b^q \approx \frac{1}{27} N_c N_f T^3 \left[\frac{\mu_b}{T} \right]. \quad (35)$$

We discussed in our previous paper how this difference in baryon-number density might lead to an isothermal baryon-number fluctuation.⁵ We suggested that if the comoving velocity of the phase boundary falls to zero, the bubbles of quark-gluon plasma drop out of thermal equilibrium, cool and nucleate their higher baryon-number concentration given in Eq. (34). We will discuss another fluctuation-generating mechanism in detail in the next section. If we define

$$R \equiv (n_b^q/n_b^h), \quad (36)$$

where the ratio of baryon-number densities is to be taken immediately after decoupling of the bubbles of quark-gluon plasma, or in the manner described in Sec. IV, then R is a measure of the amplitude of the isothermal baryon-number fluctuations. For the chemical equilibrium limit discussed above, fluctuations with amplitudes

$$R \approx \frac{2}{9} \left[\frac{\pi^3}{8} \right]^{1/2} \left[\frac{T_c}{m} \right]^{3/2} e^{m/T_c} \quad (37)$$

are produced. Inclusion of other baryonic resonances expected to be in equilibrium in the hadron soup tends to decrease the value R by providing a higher statistical weight for baryon number in the hadron phase. This effect is smallest at low temperature where, as we see from Eq. (37), R will be largest. Figure 7 gives this equilibrium amplitude R as a function of T_c , including the hadronic resonances. As we showed in our previous paper, when $T_c < 125$ MeV and $R \geq 20$ these fluctuations will have a significant influence on nucleosynthesis. The difference in baryon-number concentration in the two

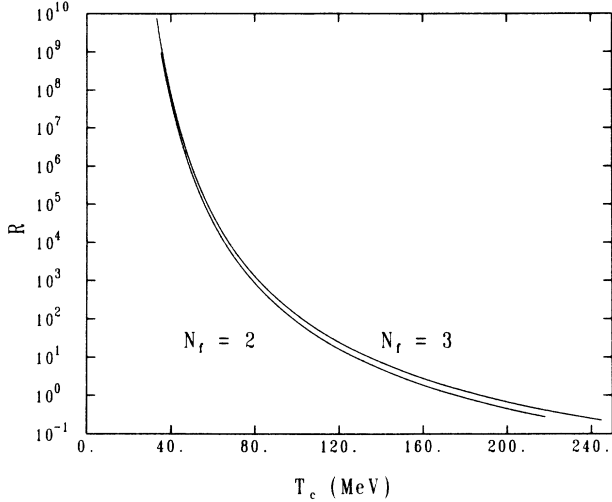


FIG. 7. The equilibrium baryon-number density ratio R as a function of coexistence temperature T_c . Curves are given for two and three relativistic quark flavors.

phases results from the difference in the mass of the particles which carry baryon number: nonrelativistic neutrons, protons, and other baryons on the one hand, and relativistic quarks on the other. We will discuss below the case where the particles which carry baryon number in the high-temperature phase (or quark phase) are nonrelativistic.

The amplitudes of isothermal baryon-number fluctuations generated in the chemical equilibrium limit are lower limits to the values obtained when the actual baryon-number transport processes are considered. The baryon content of the Universe is initially in the shrinking bubbles of the high-temperature phase, so that unless the baryon transport rate is efficient, chemical equilibrium will never be reached. The amplitude of the resulting fluctuations at phase decoupling will again be given by the ratio of Eqs. (35) and (34), but where now the two phases will each have different μ_b .

Consider the following phase-space argument for the baryon-number transport rate across a front separating a deconfined quark-gluon plasma from a gas of hadrons at the same temperature. We first consider transport from the unconfined to the confined phase. From Eq. (6b) the number density of quarks is

$$n_q \simeq 0.278g\alpha T^3, \quad (38)$$

where g is the statistical weight, so that for quarks of a given flavor and color, $g = 1$, and for all colors and flavors $g = 2n_f n_c$. The recombination rate per unit area at the front including both baryons and antibaryons is defined as

$$\Lambda \equiv f \Sigma_Q, \quad (39)$$

where f is the net flux of quarks and Σ_Q is the probability of combining three quarks at the front into a color singlet, either a baryon or antibaryon. Clearly since Σ is related to the probability of finding three quarks of the

right color and flavor in 1 fm^3 in 10^{-23} s , it must depend on the cube of the quark number density. We derive, for this probability,

$$\Sigma_Q \equiv (1.38 \times 10^{-5}) \Sigma_q \left[\frac{T}{100 \text{ MeV}} \right]^9, \quad (40)$$

where Σ_q is the dimensionless transmission probability through the phase boundary, such that $\Sigma_Q = 1$ corresponds to unit probability for recombination. We will use detailed balance below to argue what the appropriate value of Σ_q should be in terms of a similarly defined Σ_h , the baryon phase-boundary transmission probability. The total baryon recombination rate per unit area of the boundary is then

$$\Lambda \approx 3.3 \times 10^{42} (\text{cm}^{-2}\text{s}^{-1}) \left[\frac{T}{100 \text{ MeV}} \right]^{12} \Sigma_q. \quad (41)$$

The net baryon-number transport rate across the front is

$$\Lambda_q = \Lambda \xi, \quad (42a)$$

where ξ is the net number of quarks over antiquarks divided by the total number of quarks of all kinds,

$$\xi \equiv \frac{N_q - N_{\bar{q}}}{N_q^{\text{tot}}} \simeq 0.61 \mu_b / T \quad (42b)$$

so that

$$\Lambda_q (\text{cm}^{-2}\text{s}^{-1}) \simeq (2.0 \times 10^{42}) \Sigma_q \left[\frac{T}{100 \text{ MeV}} \right]^{12} \times \left[\frac{\mu_b}{T} \right]. \quad (42c)$$

The net number of baryons encountered by the front per unit area, in time Δt , as it moves from the hadron gas into the quark-gluon plasma will be

$$N_b (\text{cm}^{-2}) \simeq (2.62 \times 10^{42}) (V_f) \left[\frac{\Delta t}{10^{-6} \text{ s}} \right] \times \left[\frac{T}{100 \text{ MeV}} \right]^3 \left[\frac{\mu_b}{T} \right], \quad (43)$$

where V_f is the speed of the front in units of the speed of light. From Eq. (42c) the net baryon number recombined at the front, per unit area, in time Δt is

$$\Delta N_b (\text{cm}^{-2}) = \Lambda_q \Delta t = (2.0 \times 10^{36}) \Sigma_q \left[\frac{T}{100 \text{ MeV}} \right]^{12} \times \left[\frac{\mu_b}{T} \right] \left[\frac{\Delta t}{10^{-6} \text{ s}} \right], \quad (44)$$

so that we can define a filter factor F as the ratio of the net baryon number passed by the front to the total baryon number encountered by the front:

$$F \equiv \frac{\Delta N_b}{N_b} = (2.3 \times 10^{-6}) \left[\frac{T}{100 \text{ MeV}} \right]^9 \Sigma_q V_f^{-1} \quad (45)$$

or unity, whichever is smaller. If we take $V_f \simeq 0.1$ and $\Sigma_q \simeq 1$ then we note that $F \simeq 1$ for $T \simeq 330$ MeV. However, when the temperature is favorable for the generation of large-amplitude isothermal baryon-number fluctuations via the chemical equilibrium process, $T_c < 125$ MeV, then $F \ll 1$. In this case baryon number is not readily transported through the front.

We now consider the reverse process of baryon-number transport from the confined phase to the unconfined phase. Using the low- (μ_b/T) expression in Eq. (34) for n_b^h , the flux of baryon number directed at the wall from the hadron phase side is

$$f^h \approx 1/3 n_b^h V_b \approx \left[\frac{8}{3\pi^3} \right]^{1/2} c T^2 m \left[\frac{\mu_b}{T} \right] e^{-m/T}, \quad (46)$$

where V_b is the mean speed of a nucleon and where, explicitly, c is the speed. If the probability that a baryon gets through the phase boundary is Σ_h then the rate of baryon-number transfer per unit area from the hadron phase to the quark-gluon plasma phase is

$$\Lambda_h \approx (1.079 \times 10^{49} \text{ cm}^{-2} \text{ s}^{-1}) \left[\frac{T}{100 \text{ MeV}} \right]^2 \times \left[\frac{\mu_b}{T} \right] \exp(-938 \text{ MeV}/T) \Sigma_h. \quad (47)$$

The maximum value of the baryon transmission probability through the phase boundary is unity, corresponding to freely streaming baryons. Clearly the value of Σ_h depends on the detailed physics of the boundary; we will discuss a model for Σ_h below.

Detailed balance can be used to get the ratio of Σ_q/Σ_h . In equilibrium the baryon chemical potentials in the two phases on either side of the boundary wall are equal and the net baryon-number transfer rate across the wall must vanish, so that $\Lambda_h = \Lambda_q$. Using Eqs. (42c) and (47) these equilibrium conditions give

$$\Sigma_q \approx (5.4 \times 10^6) \left[\frac{T}{100 \text{ MeV}} \right]^{-10} \times \exp \left[\frac{-938 \text{ MeV}}{T} \right] \Sigma_h. \quad (48)$$

Using this value of Σ_q in Eq. (45) gives the filter factor

$$F \approx (1239) \Sigma_h \left[\frac{\text{MeV}}{T} \right] \exp \left[\frac{-938 \text{ MeV}}{T} \right] V_f^{-1}, \quad (49)$$

where V_f is the speed of the phase boundary wall in units of c .

The baryon-number density in each phase can be followed in time as the baryon number moves across the phase boundary. If n_b^h and n_b^q are the net baryon-number densities in the hadron and quark-gluon plasma phases, respectively, then

$$\dot{n}_b^q = -n_b^q \lambda_q + n_b^h \lambda_h - n_b^q \left[\frac{\dot{V}}{V} + \frac{\dot{f}_v}{f_v} \right], \quad (50a)$$

$$\dot{n}_b^h = \left[\frac{f_v}{1-f_v} \right] \left[-n_b^h \lambda_h + n_b^q \lambda_q + n_b^h \frac{\dot{f}_v}{f_v} \right] - n_b^h \frac{\dot{V}}{V}, \quad (50b)$$

where \dot{n}_b^q and \dot{n}_b^h are the time rates of change baryon-number density in each phase, λ_q and λ_h are characteristic baryon-number transfer rates from quark-gluon plasma to hadron phase and the reverse, respectively. The last terms in Eqs. (50a) and (50b) are volume red-shift factors:

$$\frac{\dot{V}}{V} = \frac{3\dot{A}}{A}, \quad (50c)$$

where the volume element is $V = V_0 (A/A_0)^3$ and \dot{A}/A can be found from Eqs. (29) and (32a). The total baryon number per comoving volume $V = V_0 (A/A_0)^3$ is constant at N_0 :

$$\frac{N_0}{V} = n_b^q f_v + n_b^h (1-f_v). \quad (51)$$

The total baryon number swept up by the wall in the quark-gluon phase, and pushed through to the hadron phase, divided by the total volume in the quark phase is

$$n_b^q \lambda_q = 4\pi r^2 N_n \frac{V_0}{f_v V} V_f F, \quad (52a)$$

where r is the typical bubble radius, N_n is as in Eq. (33a), and V_0 is the horizon volume at the end of the nucleation epoch. Using the value of the filter factor F from Eq. (49) it can be shown that

$$\lambda_q \approx (1.115 \times 10^{14} \text{ s}^{-1}) \left[\frac{\text{MeV}}{T_c} \right] \times \exp \left[\frac{-938 \text{ MeV}}{T_c} \right] \left[\frac{\text{cm}}{r} \right] \Sigma_h, \quad (52b)$$

where we have made use of an approximation for f_v , is

$$f_v \approx \frac{4}{3} \pi r^3 N_n \frac{V_0}{V}, \quad (53)$$

when $f_v \leq 0.5$.

By reasoning similar to that employed above it can be shown that

$$n_b^h \lambda_h = \frac{1}{3} n_b^h V_b \left[\frac{4\pi r^2 N_n V_0}{f_v V} \right] \Sigma_h, \quad (54a)$$

where V_b is a typical thermal velocity for a nucleon, $V_b \approx (3T/m)^{1/2}$, from which we derive

$$\lambda_h \approx (1.70 \times 10^9 \text{ s}^{-1}) \left[\frac{T_c}{\text{MeV}} \right]^{1/2} \left[\frac{\text{cm}}{r} \right] \Sigma_h. \quad (54b)$$

The first-order differential equations for n_b^q and n_b^h [Eqs. (49a) and (49b)] and the constraint [Eq. (51)] are easily integrated. In the limit of a static universe, $\dot{V}/V = 0$, which corresponds to a static phase boundary, after a sufficiently long time $t \gg \lambda_h^{-1}$ we obtain the equilibrium baryon-number density ratio,

$$\left(\frac{n_b^g}{n_b^h} \right)_{\text{eq}} = \frac{\lambda_h}{\lambda_q}, \quad (55)$$

which is the same ratio given in Eq. (37). In the expanding Universe case, Figs. 8(a)–8(d) present the ratio $R = n_b^g/n_b^h$ as a function of time from the onset of the constant-temperature epoch to the end of the phase transition. Figure 8(a) corresponds to $T_c = 100$ MeV, while Figs. 8(b)–8(d) correspond to $T_c = 120, 150,$ and 200 MeV, respectively. The baryon-number density ratio R is computed at each T_c for several values of the nucleon transmission probability: $\Sigma_h = 1, 10^{-2}, 10^{-3}, 10^{-4}, 10^{-5},$ and 10^{-6} . We note that for $\Sigma_h = 1$, baryon-number chemical equilibrium is rapidly established, with R being driven to the equilibrium value [Eq. (37)] on a time scale short compared to either the Hubble time or the duration

of the constant-temperature epoch. For $\Sigma_h \ll 1$ chemical equilibrium is not obtained and R can be much larger than R_{eq} .

What is the appropriate value of the baryon transmission probability, Σ_h ? The answer to this question depends on the nature of the phase boundary separating the confined vacuum from the unconfined vacuum. Any calculation of Σ_h , therefore, will be highly model dependent.

If the simple baglike approach to treating the unconfined medium is taken seriously then we would expect the boundary separating the phases to behave much as the surface of a nucleon: inside, in the “unconfined” vacuum, the quarks have zero mass and the color-dielectric constant is unity, $\kappa_{\text{in}} = 1$; outside, in the “confined” vacuum, the color-dielectric constant would be zero, $\kappa_{\text{out}} \rightarrow 0$, and the bare-quark mass g^2/κ_{out} would

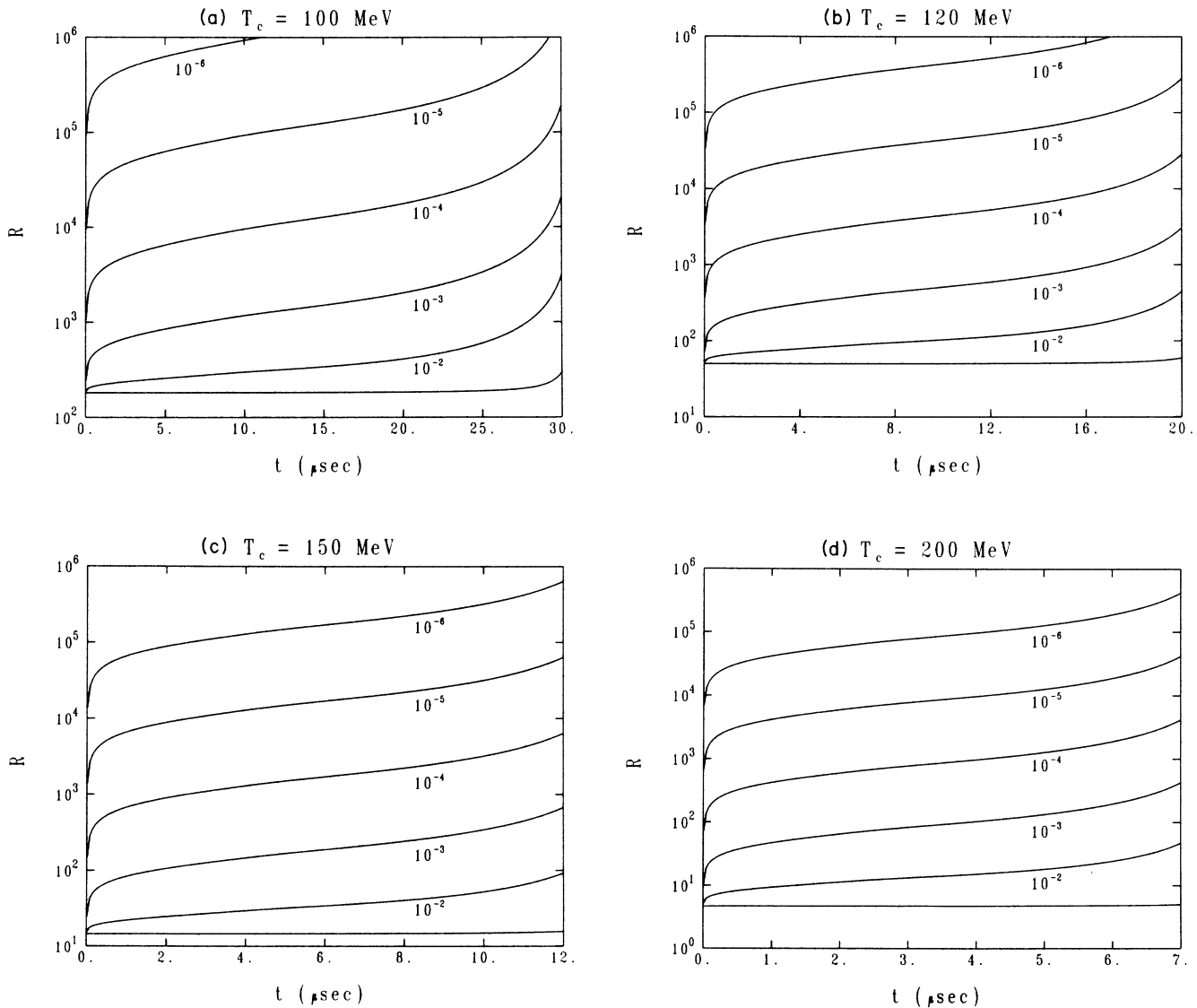


FIG. 8. The baryon-number ratio R as a function of time during the constant temperature coexistence epoch. Curves are labeled by the value of the nucleon transmission probability through the phase boundary Σ_h . The lowest curve corresponds to $\Sigma_h = 1$; the others to $\Sigma_h = 10^{-2}, 10^{-3}, 10^{-4}, 10^{-5}, 10^{-6}$. Results are given for coexistence temperature T_c of (a) $T_c = 100$ MeV; (b) $T_c = 120$ MeV; (c) $T_c = 150$ MeV; and (d) $T_c = 200$ MeV.

tend to infinity. Such schematic models for the nucleon surface have been considered in the soliton bag model,³⁶ for instance.

Consider a nucleon approaching the phase boundary. Away from the boundary the mass of the nucleon is essentially the kinetic energy of the quarks inside. When the nucleon touches the phase boundary a massless quark inside the nucleon may move through the wall into the unconfined quark-gluon plasma, leaving behind a colored object in the hadron phase with a divergent mass. If the two remaining quarks move through the wall, the energy of the configuration decreases to the original kinetic energy of the quarks. If a quark moves from the unconfined vacuum back into the "nucleon," to form a color singlet, then the energy is again reduced to its original value if the nucleon now rebounds from the wall back into the hadron phase.

In this picture the energy of the nucleon at the phase boundary can be modeled as δ -function potential, $V(x) \equiv \alpha V_0 \delta(x)$, where α has the dimensions of length and $x=0$ corresponds to the position of the bubble wall. The calculation of Σ_h is then reduced to the calculation of the nucleon tunneling probability through $V(x)$.

The parameters α and V_0 can be estimated from the surface energy in the soliton bag model: $E_s \simeq 4\pi R^2 \sigma_0^3$, where R is the radius of a nucleon and σ_0 is the characteristic mass of the confining field (the vacuum expectation value of the Higgs field associated with the confining potential). This characteristic mass is $\sigma_0 \simeq 30$ GeV (Ref. 36). Integrating the energy per unit volume, $V_0 \alpha^{-2} \delta(x)$, over the nuclear volume and identifying the surface term then yields $\alpha V_0 \sim 1$ or

$$\alpha V_0 \approx (1.2 \times 10^8 \text{ MeV fm}^{-2}) \alpha^3. \quad (56)$$

If α is taken to be twice the nucleon surface "thickness" σ_0^{-1} , then $\alpha V_0 \approx 1.6 \times 10^3$ MeV fm. The probability of a nonrelativistic nucleon of wave number k tunneling through the barrier is

$$\Sigma_h = [1 + (m\alpha V_0/k)^2]^{-1}, \quad (57)$$

where m is the mass of the nucleon. Taking a thermal average over a nonrelativistic distribution of nucleon velocities yields

$$\langle \Sigma_h \rangle \approx \left(\frac{m}{2\pi T_c} \right)^{1/2} \int_0^\infty dv_x \frac{e^{-(m/2T_c)v_x^2}}{1 + (m\alpha V_0/v_x)^2} \quad (58a)$$

$$\approx \frac{1}{2(\alpha V_0)^2} \left(\frac{T_c}{m} \right) \approx 10^{-3} \text{ at } T_c = 100 \text{ MeV}, \quad (58b)$$

where v_x is the velocity of the nucleon toward the wall. Note that the nucleon transmission probability depends only linearly on temperature but quadratically on the rather uncertain barrier parameters α and V_0 . The value of $\langle \Sigma_h \rangle$ may be orders of magnitude larger or smaller than indicated by this rough estimate. We emphasize that the schematic bag-model approach to treating the phase boundary may be inappropriate and, hence, we treat Σ_h as a free parameter.

VI. GENERATION OF ISOTHERMAL BARYON-NUMBER FLUCTUATIONS

The basis for isothermal baryon-number fluctuation generation lies in the difference in baryon-number concentration between the unconfined and confined phases; $R = n_g^q/n_b^h$. The preceding section showed that R can be much larger than unity, even in the limit of baryon chemical equilibrium; if equilibrium is not established across the phase boundary then R is larger than the equilibrium value.

If at any point during the shrinking of the bubbles of quark-gluon plasma the release of latent heat is not rapid enough to compensate for the universal expansion then the temperature of the bubbles will fall below T_c and nucleation of the concentrated baryon number will follow. This cooling process has been considered by Applegate and Hogan.⁷ The amplitude of the resulting isothermal baryon-number fluctuations has been considered in our previous paper.⁵

We now demonstrate that isothermal baryon-number fluctuations are produced so long as $R > 1$, even in the limit where the phase transition goes to completion during the constant-temperature epoch. The integration of the baryon-number transport Eqs. (49a) and (49b) shows that the local baryon-number densities on either side of the phase boundary rapidly approach a nearly constant ratio R : either the equilibrium R or one somewhat larger due to the filtering effect of the wall, as shown in Figs. 8(a)–8(d). This ratio is approached on a time scale short compared to the duration of the constant-temperature epoch due, essentially, to the large coefficients of the rates λ_q and λ_h in Eqs. (52b) and (54b), respectively.

The mean free path of a nucleon in the hadron phase was discussed in Sec. III, where it was shown that in a Hubble time a nucleon, or any hadronic state carrying baryon number, would move only 10^{-3} cm. This distance is small compared to the proper distance through which a typical bubble wall moves during the constant-temperature epoch, ~ 5000 cm. Even if one-gluon-exchange effects are taken into account the baryon (quark) mean free path in the unconfined phase will be large compared to that in the confined phase.

These considerations suggest a simple model for a shrinking bubble of quark-gluon plasma which is similar to that of Applegate and Hogan.⁷ First, since the neutrino mean free path is large, we argue that the latent heat liberated by the spherical shell of volume converted from unconfined to confined vacuum by the movement of the phase boundary will be rapidly communicated throughout the volume of the shrinking bubble, keeping the unconfined medium near T_c and guaranteeing that the bubble does not nucleate and shrinks away to nothing. A second point is that this spherical shell of new vacuum contains no initial baryon number. Baryon number must either leak in from a previous shell converted to the confined phase or be transported across the phase boundary from the unconfined phase. The former process must be slow because of the small baryon mean free path; on the other hand, we have argued above that the latter process is rapid and that baryon-number density on

either side of the front will be driven rapidly to the ratio R . As the bubble of quark-gluon plasma shrinks the baryon-number, concentration inside, n_b^g , increases and hence the baryon-number density in the hadron shell surrounding the bubble,

$$n_b^h = n_b^g / R, \quad (59)$$

increases as well. After the bubble of quark-gluon plasma has shrunk away it leaves a fossil isothermal baryon-number fluctuation: each successive "shell" of hadronic material left by the bubble has larger baryon-number density.

If V is a representative volume of the Universe then $n_b^g f_v V$ is the total baryon number in the unconfined phase. As the bubble shrinks it loses a shell of volume $d(f_v V)$ to the confined phase and hence it loses baryon number,

$$d(n_b^g f_v V) = (n_b^g / R) d(f_v V), \quad (60)$$

to the hadron shell. The time evolution of the baryon density in the quark-gluon plasma bubble is then given by

$$\frac{dn_b^g}{dt} = -n_b^g(1 - 1/R) \left[\frac{\dot{f}_v}{f_v} + \frac{\dot{V}}{V} \right], \quad (61a)$$

where the notation is as in earlier sections and

$$n_b^g(t) = n_b^g(0) \left[\frac{V}{V_0} f_v \right]^{1/R - 1}, \quad (61b)$$

where $t=0$ is the end of the nucleation epoch, $n_b^g(0)$ is the initial baryon-number concentration, and where the initial volume in question is V_0 . The equivalent baryon-number density in the hadron phase is given by Eq. (59) at any time t . Since f_v and $V/V_0 = (A/A_i)^3$ are known functions of time, Eq. (61b) can be used to find the baryon-number distribution in the fossil fluctuation:

$$\frac{dn_b}{df_v} = \frac{4}{3} \pi \left[\frac{-n_b^g(0)}{xR} \right] \frac{1}{f_v}, \quad (62a)$$

where x is the statistical weight ratio as previously defined. This distribution can also be written in terms of the proper radius r of the fluctuation:

$$\frac{dn_b}{dr} = 4\pi \left[\frac{-n_b^g(0)}{xR} \right] \frac{1}{r}. \quad (62b)$$

This is similar to the result in Ref. 7. Note that a large baryon-number ratio R has the effect of narrowing the isothermal baryon-number fluctuation peak.

The above discussion of the shape of the fluctuations depends on three assumptions. The first is that the baryon-number distribution in the quark-gluon plasma is uniform and that baryon number does not "pile up" at the phase boundary. This assumption is equivalent to the statement that the mean free path of a quark in the unconfined medium is large. This is clearly a model-dependent result. The second assumption is that the baryon number in the hadron phase does not significantly diffuse on the time scale of the duration of the constant-

temperature coexistence epoch. Arguments based on the nucleon mean free path were used to justify this assumption. Finally, we have assumed that there are no large-scale streaming effects which might smear out the fluctuation shape. Fluid velocities in the limit where all enthalpy transport is by hydrodynamic flows have been estimated.⁷ The smearing introduced would be of the same order as by proton diffusion after weak decoupling.

Finally, the fluctuation shape is modified after weak decoupling by the differential diffusion of neutrons and protons.⁷ The effect of these modified fluctuations on big-bang nucleosynthesis is discussed below.

VII. BARYON DENSITY FLUCTUATIONS AND PRIMORDIAL NUCLEOSYNTHESIS

The isothermal baryon-number density fluctuations discussed in this paper can have interesting effects on primordial nucleosynthesis. There are two influences which must be considered. One is the fact that more than one baryon to photon ratio must be averaged to produce the final nucleosynthetic yield. Such an averaging by itself can significantly alter the yields from primordial nucleosynthesis.⁴ The second intriguing effect³ is that the neutron and proton components of these density fluctuations will diffuse differently after the weak reactions fall out of equilibrium. Essentially, the neutron collision mean free path is much larger (by more than an order of magnitude) than the proton mean free path since the neutron only interacts with the background plasma via nucleon scattering or via the small neutron dipole moment. The diffusion of protons, on the other hand, is slowed by the more dominant proton-electron scattering. This diffusion of neutrons leads to a filling of the low-density voids between the high-density fluctuations with neutron-rich material. The high-density regions are correspondingly proton-rich relative to standard big-bang nucleosynthesis.¹⁷

In the work of Applegate, Hogan, and Scherrer,³ the nucleosynthesis in the low-density neutron-rich regions was explored as a function of the fraction of neutrons which diffuse into the low-density regions, and the volume fraction occupied by these neutrons. In our previous work⁵ we considered nucleosynthesis in both the proton- and neutron-rich phases as a function of their relative volume fractions for a single fixed ratio of baryon densities between the two regions, normalized such that $\Omega_b = 1$. We discovered that significant nucleosynthesis also occurs in the proton-rich phase, particularly for ${}^7\text{Li}$. This leads to an overproduction of ${}^7\text{Li}$ when the two regions are averaged, although the other abundances were reasonably well reproduced in a universe with $\Omega_b = 1$. It was also discovered that the production of heavy elements with $A \geq 12$ was not as efficient as first proposed.³ In this work we extend our study to consider the effects of these baryon inhomogeneities in a Universe with $\Omega \neq 1$, and as a function of the ratio of the baryon densities in the two phases. (This latter parameter is related to the coexistence temperature during the phase transition.) Our aim is to delimit the parameter space of this model which is consistent with the constraints from light-

element abundances.

For the purposes of this parameter study we utilize the two-zone complete diffusion scenario discussed in Ref. 5 which reduces the parameter space to three quantities, the total average baryon density Ω_b , the ratio of densities in the two regions R , and the volume fraction f_v , in the high-density regions just before nucleosynthesis. We will also utilize the fluctuation profile computed in the previous section.

The effects of nucleon diffusion in this model are included by assuming (1) that the nucleation rate is sufficiently great that the mean separation between fluctuations is significantly less than a neutron diffusion length at the time of nucleosynthesis, and (2) that the proton diffusion can be ignored. These assumptions are a fair approximation to the results of our nucleation rate studies discussed above and to the diffusion rates of Ref. 3.

To implement these assumptions we have utilized the big-bang nucleosynthesis code of Wagoner¹⁷ with three neutron flavors, a neutron half-life of 10.6 min, and a number of nuclear reactions updated from the original version. We note that the conversion from baryon-to-photon ratio to Ω_b in what follows is based upon assumed values for the present cosmic background radiation temperature of 2.7 K and the Hubble constant of 50 km sec⁻¹Mpc¹. We begin the nucleosynthesis calculations with relative baryon densities in the high- and low-density regions (Ω_h or Ω_l) as a function of f_v and average Ω :

$$\Omega_h = \frac{\Omega R}{f_v(R-1) + 1}, \quad (63a)$$

$$\Omega_l = \Omega_h / R. \quad (63b)$$

We assume that the neutron diffusion occurs between the freeze-out of the weak reactions (at $T \approx 1.3 \times 10^9$ K, 0.11 MeV) and the onset of nucleosynthesis (at $T \approx 0.9 \times 10^9$ K) about 100 s later. Note that by weak “freeze-out” we mean that temperature at which free neutron decay dominates all other $n \leftrightarrow p$ reactions. The weak interaction drops out of equilibrium at a much higher temperature, $T \leq 1$ MeV, when typical weak rates become small compared to the universal expansion rate. The assumption of neutron diffusion equilibrium near $T \approx 1.3 \times 10^9$ K depends upon what one takes to be the mean separation between nucleation sites. If the density of nucleation sites is high, the physical size of the fluctuations will be small compared to the neutron diffusion length. Therefore, the neutron density will equilibrate at a temperature closer to the temperature at which weak reactions fall out of equilibrium ($\approx 10^{10}$ K) when the neutron mass fraction is higher. However, if the size of the fluctuations is small during nucleosynthesis, neutrons can quickly diffuse back into the high-density zones as they are depleted in those regions by nuclear reactions. This would result in nucleosynthetic yields similar to those of the standard big bang. The most favorable case for inhomogeneous nucleosynthesis occurs for fluctuation sizes sufficiently large that neutron equilibrium is not achieved until just before nucleosynthesis and the effect of the flow of neutrons

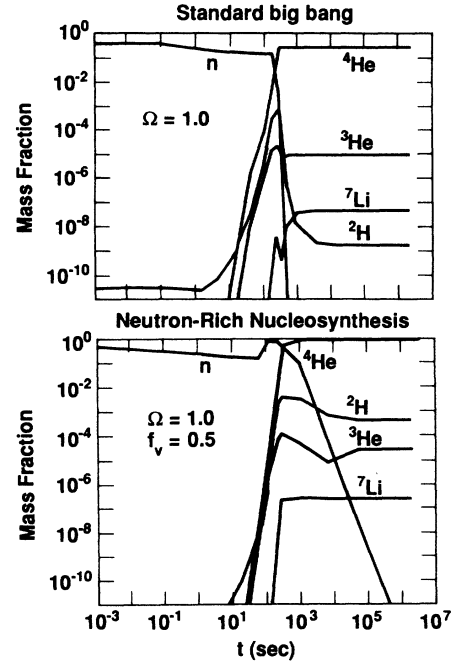


FIG. 9. Big-bang nucleosynthesis yields as a function of time in an $\Omega_b = 1.0$ universe for (a) the standard big bang and (b) the neutron-rich low-density regions in an inhomogeneous universe with fluctuation amplitude, $R = 50$, and in which half of the volume is in the low-density regions.

back into the high-density zones is diminished. We will discuss the details of the coupling between neutron diffusion and nucleosynthesis in a forthcoming paper. Since one of our purposes in this work is to establish upper limits upon the phase transition physics from the nucleosynthesis, we utilize this most optimistic model for neutron diffusion and nucleosynthesis.

As nucleosynthesis begins after neutron diffusion, the Universe consists of a high baryon density proton-rich region, (1) with

$$\Omega^{(1)} = X_n \Omega + \Omega_h (1 - X_n), \quad (64)$$

$$X_n^{(1)} = X_n / \Omega^{(1)}, \quad (65)$$

where X_n is the neutron mass fraction before nucleon diffusion at $T = 1.3 \times 10^9$ K, and a low baryon density neutron-rich region and (2) with

$$\Omega^{(2)} = X_n \Omega + \Omega_l (1 - X_n), \quad (66)$$

$$X_n^{(2)} = X_n / \Omega^{(2)}. \quad (67)$$

The final averaged mass fractions for each nuclide are then

$$\bar{X}_i = \frac{f_v X_i^{(1)} \Omega^{(1)} + (1 - f_v) X_i^{(2)} \Omega^{(2)}}{f_v \Omega^{(1)} + (1 - f_v) \Omega^{(2)}}. \quad (68)$$

Figures 9(a) and 9(b) show a history of nucleosynthesis in the standard big-bang compared with the neutron-rich regions in a Universe with average $\Omega_b = 1$ and $R = 50$. These figures illustrate the dramatic effect of the baryon diffusion on primordial nucleosynthesis. In the standard

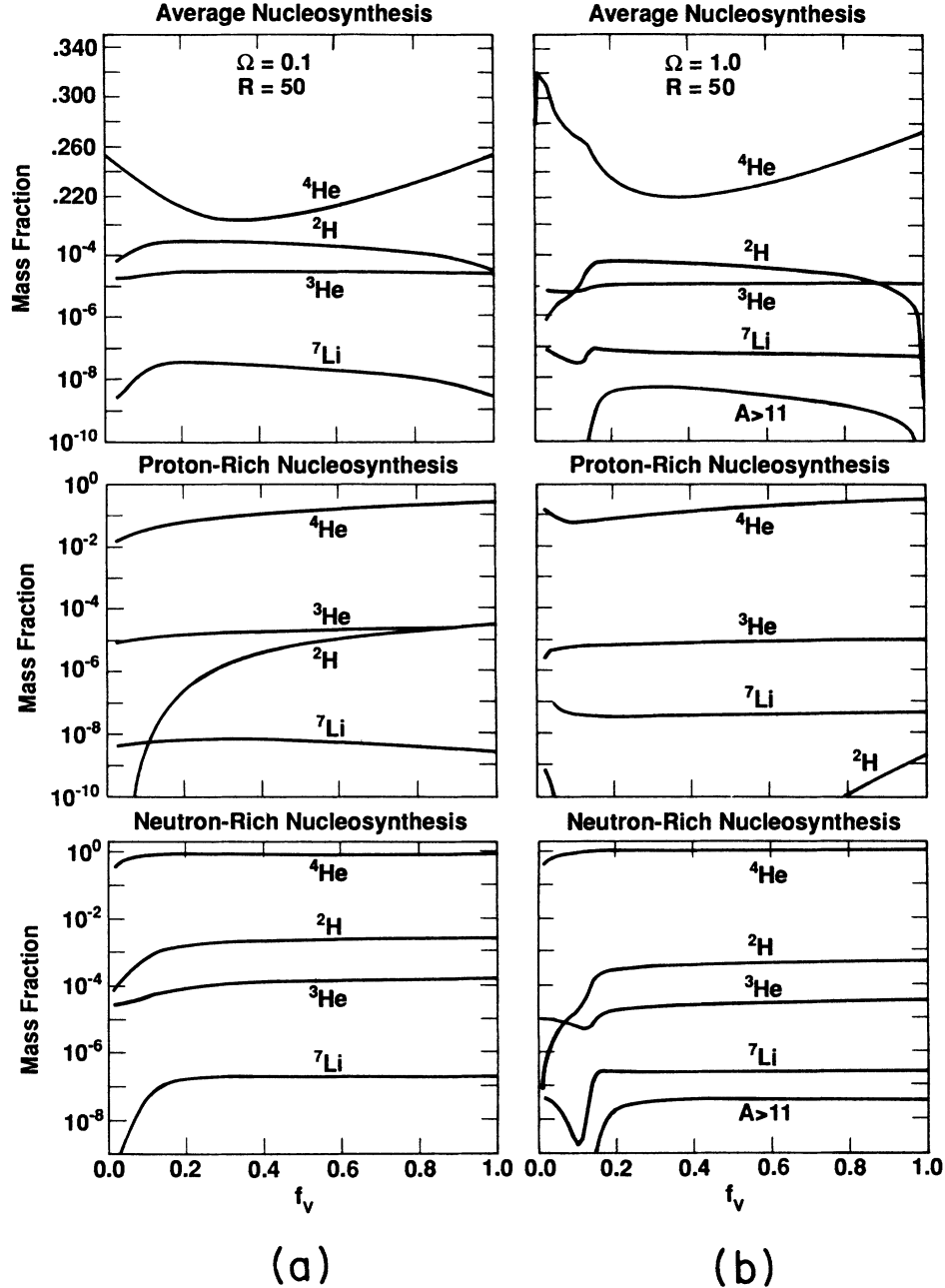


FIG. 10. Primordial nucleosynthesis for the high- and low-density regions and their average yields as a function of volume fraction f_v for a fixed fluctuation amplitude, $R = 50$, and with (a) $\Omega_b = 0.1$, (b) $\Omega_b = 1.0$. Note that the average yields for ${}^2\text{H}$ are relatively insensitive to Ω_b . Note also that the yields do not depend much on f_v for most of the range $0.2 \leq f_v \leq 0.8$.

big bang, at high baryon densities, essentially all of the available neutrons are quickly converted into ${}^4\text{He}$ at $t \sim 100$ s. In the low-density regions, the neutron mass fraction is set to close to unity when the baryon diffusion is turned on at $t \sim 50$ s. It is then the proton mass fraction which is absorbed to make ${}^4\text{He}$. Further ${}^4\text{He}$ production must await the decay of neutrons into protons. Thus, there is a significant neutron mass fraction until much later times. ${}^2\text{H}$ is therefore produced at lower densities and survives further nuclear reactions. Since ${}^3\text{H}$, ${}^3\text{He}$, and ${}^4\text{He}$ are large, there is also significant production of ${}^7\text{Li}$ in these regions.

In Figs. 10(a) and 10(b) we show averaged nucleosynthesis yields and nucleosynthesis in the proton- and neutron-rich regions for $\Omega = 0.1$ and 1.0 when $R = 50$. This corresponds to the ratio of baryon densities for chemical equilibrium when the coexistence temperature is 110 MeV with three relativistic quark flavors, or when $T_c > 110$ MeV and $\Sigma_h < 1$. The intriguing feature of these results is that, for $\Omega_b = 1$, over a broad range for the parameter f_v , the main abundance constraints from primordial nucleosynthesis (i.e., ${}^4\text{He}$ and ${}^2\text{H}$) can be satisfied. There is, however, a slight underproduction of ${}^3\text{He}$ and a larger overproduction of ${}^7\text{Li}$. This overproduction of ${}^7\text{Li}$

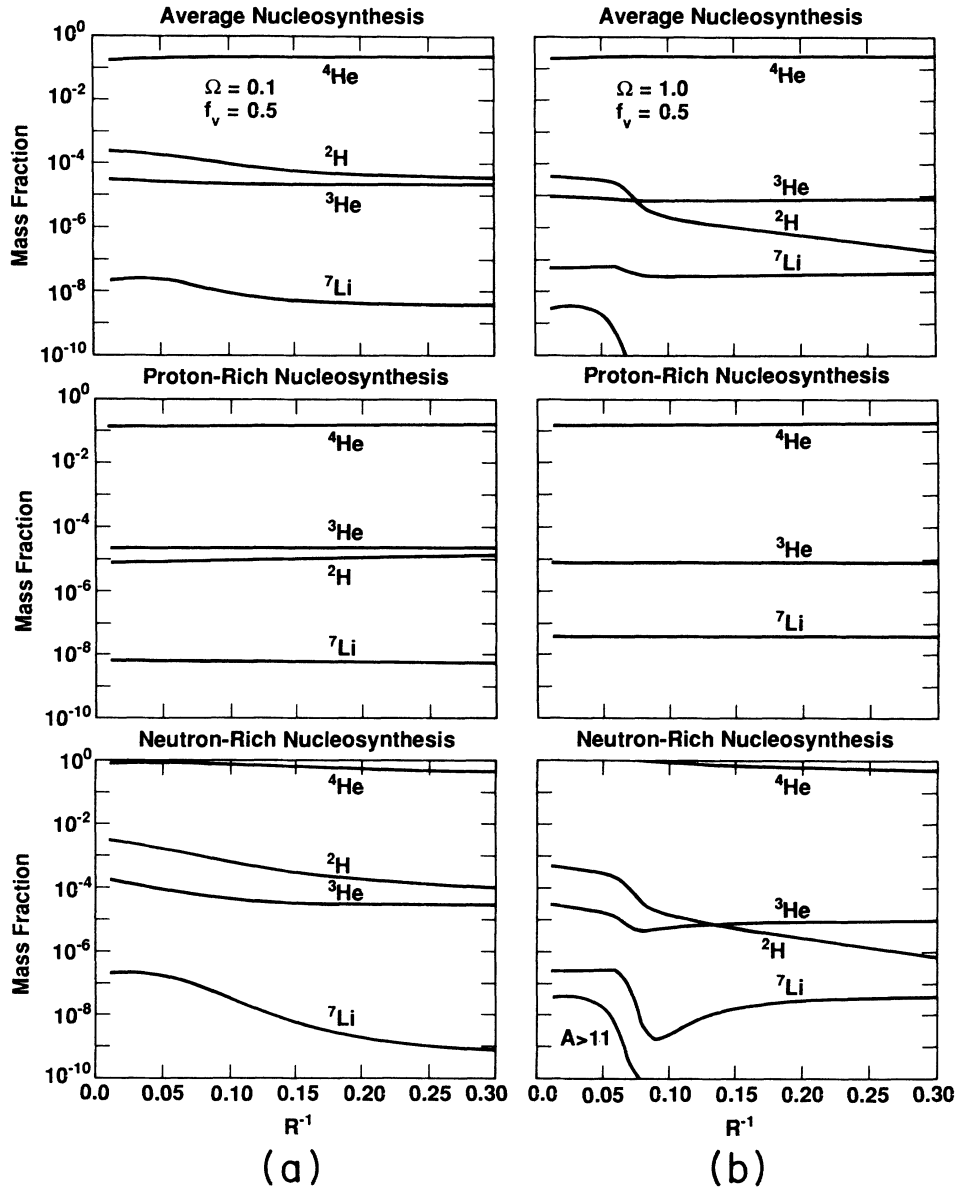


FIG. 11. Primordial nucleosynthesis yields in the high- and low-density regions and their average as a function of universe fluctuation amplitude $1/R$ for $f_v=0.5$ and (a) $\Omega_b=0.1$, (b) $\Omega_n=1.0$. Note that for $R > 20$, all yields become virtually independent of the fluctuation amplitude.

is due to the fact that ${}^7\text{Li}$ can be produced in significant amounts in both the neutron- and proton-rich regions. However, this overabundance may not be too significant due to the uncertainties³⁷ in the ${}^7\text{Li}$ abundance, the nuclear reaction rates, and stellar destruction of ${}^7\text{Li}$. Nevertheless, this overabundance appears to be an unavoidable consequence of these models due to the large contribution from the ${}^3\text{He}(\alpha, \gamma){}^7\text{Be}$ reaction in the high baryon density regions and the ${}^3\text{H}(\alpha, \gamma){}^7\text{Li}$ reaction in the low baryon density regions. This seems to be a general problem with nucleosynthesis in inhomogeneous cosmologies, unless the high baryon density regions selectively collapse to form cold dark matter.⁴

In Figs. 10(a) and 10(b) there is little dependence of the average ${}^7\text{Li}$ mass fraction with f_v , although ${}^2\text{H}$ decreases dramatically when f_v is near the extrema, $f_v=0$ or 1,

where the results of standard big-bang nucleosynthesis are reproduced. For this reason we restrict our discussion to the f_v in the range $f_v=0.5\pm 0.4$ for which the abundances are largely insensitive to f_v and there is sufficient production of ${}^2\text{H}$.

Figures 11(a) and 11(b) illustrate how the nucleosynthesis yields vary as a function of R for fixed f_v and $\Omega_b=1.0$ and 0.1 . In order to exaggerate the structure in these figures, yields are plotted as a function of $1/R$. Note, however, for $R > 20$ ($1/R < 0.05$) the yields become essentially independent of fluctuation amplitudes. Typically the average ${}^7\text{Li}$ and ${}^2\text{H}$ mass fractions can increase by as much as an order of magnitude over the interval of $R=1\rightarrow 20$. (Note that $R=1$ corresponds to standard big-bang nucleosynthesis with no neutron diffusion.) The slight increase for both ${}^7\text{Li}$ and ${}^2\text{H}$ with

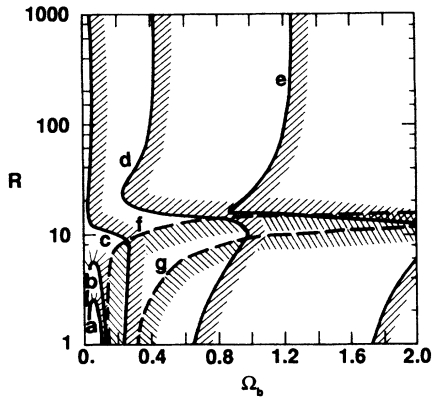


FIG. 12. Regions of the R - Ω_b plane which are consistent with the ${}^7\text{Li}$ and ${}^2\text{H}$ abundances. The solid lines denote regions allowed by the ${}^7\text{Li}$ abundance corresponding to upper limits taken from (a) ${}^7\text{Li}/\text{H} < 1.8 \times 10^{-10}$ (Pop II halo abundance); (b) ${}^7\text{Li}/\text{H} < 8 \times 10^{-10}$ (Pop I disk abundance); (c) ${}^7\text{Li}/\text{H} < 2.6 \times 10^{-9}$ (CCI meteoritic abundances); (d) ${}^7\text{Li}/\text{H} < 8 \times 10^{-9}$; (e) ${}^7\text{Li}/\text{H} < 8 \times 10^{-9}$ (astration factor = $10 \times$ Pop I abundance). The dashed lines are from the lower limit to the ${}^2\text{H}$ abundance; (f) $D/\text{H} > 10^{-5}$; (g) $D/\text{H} > 10^{-6}$.

increasing R is basically due to the fact that the relative baryon density in the low-density neutron-rich region decreases with R . For $\Omega_b = 1$, one can see the effect of the minimum in ${}^7\text{Li}$ production as a function of baryon density due to the increased ${}^7\text{Li}$ destruction before ${}^7\text{Be}$ production from the ${}^3\text{He}(\alpha, \gamma){}^7\text{Be}$ reaction.

To illustrate the effect of a distribution of baryon densities rather than the two-zone model considered above, we have also calculated abundances in a Universe with the continuous distribution of baryon densities given by Eq. (62a), $dn_b/df_v \propto 1/f_v$, with R normalized such that $\Omega = 1$. This calculation yields ${}^4\text{He}/\text{H} = 0.275$, ${}^2\text{H}/\text{H} = 7.2 \times 10^{-6}$, ${}^3\text{He} = 6.1 \times 10^{-6}$, and ${}^7\text{Li} = 3.5 \times 10^{-8}$, with $A \geq 12$ nuclei $< 5 \times 10^{-11}$. These results are outside the range of acceptable light-element abundances, which suggest that the constraints on isothermal baryon-density fluctuations from the quark-hadron phase transition may even be more severe when a realistic distribution of baryon densities is taken into account. Nevertheless, this result is inconclusive since the $1/f_v$ distribution is over simplistic for the reasons given above. We will consider more realistic fluctuation spectra coupled with hydrodynamic flows and baryon diffusion in a subsequent paper.

In Fig. 12 we delimit the regions of the R - Ω_b plane which are consistent with the constraints from light-element abundances in the two-zone model. Contours are drawn on this figure which show the values of R and Ω_b which satisfy the constraint noted in the figure captions. Curves are drawn corresponding to both deuterium production and ${}^7\text{Li}$ production. Because of the large uncertainties in the primordial ${}^7\text{Li}$ abundance, contours are shown for a number of different upper limits to primordial ${}^7\text{Li}$ ranging from the lowest values from Pop II halo stars to the highest values corresponding to a large

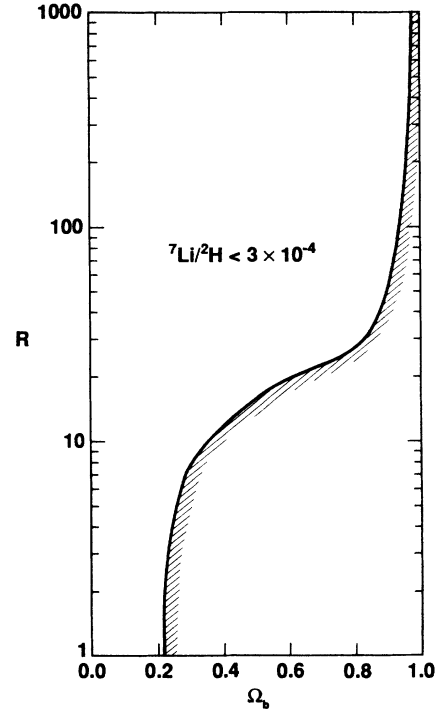


FIG. 13. Constraint on values of R and Ω_b based on an apparent upper limit to the ${}^7\text{Li}/{}^2\text{H}$ ratio of 3×10^{-4} , which to first order may be independent of astration.

fraction of the primordial abundance having been destroyed in stars. Two different ${}^2\text{H}$ constraints are shown to illustrate the sensitivity to the deuterium abundance constraint.

From this figure several interesting conclusions can be drawn. One is that the deuterium constraint can only be satisfied in an $\Omega = 1$ universe if the fluctuation amplitude, $R > 20$. Perhaps more useful is the observation that if the smallest upper limits to the ${}^7\text{Li}$ abundance are correct then this constraint can only be satisfied in a universe with $R \leq 2$, which essentially would correspond to standard big-bang nucleosynthesis without fluctuations. Thus, if the Pop II or even Pop I disk ${}^7\text{Li}$ abundances are ever accepted as firm upper limits to the primordial lithium, then one could use this constraint to set an upper limit to the magnitude of baryon density fluctuations to emerge from the quark-hadron phase transition. On the other hand, if the primordial ${}^7\text{Li}$ abundance is at least 3–5 times the meteoritic value, then this constraint could be satisfied for $R \geq 15$. This suggests that if ${}^7\text{Li}$ destruction in stars (astration) has been significant over the history of the Galaxy, then the light-element abundances could be consistent with $\Omega = 1$ in baryons.

If ${}^7\text{Li}$ has been significantly astrated then it follows that ${}^2\text{H}$ must also have been astrated since the nuclide is less tightly bound than ${}^7\text{Li}$. It is therefore encouraging that deuterium is overproduced along with ${}^7\text{Li}$ in models with $R \geq 50$. It is useful to consider the constraint based upon the ratio of ${}^7\text{Li}/{}^2\text{H}$ in which the effects of astration cancel out to first order.³⁸ By choosing the highest present-day ${}^7\text{Li}$ abundance, and the lowest deuterium

abundance a firm upper limit to this ratio can be derived (${}^7\text{Li}/{}^2\text{H} < 3 \times 10^{-4}$). The R - Ω parameter space allowed by this ratio is depicted in Fig. 13. For sufficiently large values of R it is possible to have Ω_b very close to unity and still satisfy this constraint.

We also note that the upper limit to the ${}^7\text{Li}/{}^2\text{H}$ ratio could be even higher than that used for Fig. 13. The ${}^2\text{H}$ abundance is measured in the interstellar medium. If some fraction ϕ of the interstellar gas has never been processed in stars, then the maximum possible modification of the abundance is by this factor ϕ . In contrast, the ${}^7\text{Li}$ abundance is measured in the atmosphere of stars with only lower limits measured in the interstellar medium. Since individual stars may significantly modify their ${}^7\text{Li}$ abundances, these abundances may have been reduced by factors much larger than ϕ . For this reason we are less concerned about ${}^7\text{Li}$ than the other light elements.

VIII. SUMMARY AND CONCLUSION

We have shown in this paper that isothermal baryon-number density fluctuations are a plausible and perhaps unavoidable consequence of the transition from quark-gluon plasma to confined hadronic matter. At least two mechanisms for the production of such fluctuations can be identified. We identify the coexistence temperature T_c and the nucleon domain-wall transmission probability Σ_h as the main determinants of fluctuation size. We have studied the nucleation properties of these fluctuations and find that it is also plausible that these fluctuations are spaced in such a way as to allow for a separation of neutron and proton fluids by diffusion before the epoch of nucleosynthesis. Finally, we have studied the consequence of the fluctuations and baryon diffusion on primordial nucleosynthesis. The light-element abundances for $\Omega = 1$ can be reasonably well reproduced if the fluctuations are sufficiently large. There may be, however, an overproduction of ${}^7\text{Li}$. If the smallest upper limits to the primordial ${}^7\text{Li}$ abundance are correct, then one would

conclude that the effects of isothermal baryon-number fluctuations and diffusion on the early Universe must be small. On the other hand, if ${}^7\text{Li}$ and ${}^2\text{H}$ have been significantly astrated over the history of the Galaxy, and if such astration does not lead to unacceptably low abundances for other fragile light nuclei (such as ${}^6\text{Li}$, ${}^{10,11}\text{B}$, and ${}^9\text{Be}$), then it is possible to satisfy all of the constraints from primordial nucleosynthesis and have $\Omega = 1$ in baryons.

We have shown that the light-element abundance yields from big-bang nucleosynthesis in a high baryon content universe could reproduce accepted primordial abundances, in a relatively parameter-independent way, with the exception of ${}^7\text{Li}$. The point is that the limit on Ω_b from primordial nucleosynthesis now rises or falls on the basis of what is taken to be the primordial ${}^7\text{Li}$ abundance. The measurements of the ${}^7\text{Li}$ abundances and the ${}^7\text{Li}/{}^6\text{Li}$ isotopic ratios, when coupled with self-consistent models of galactic chemical evolution, now seem to point to a low primordial Li abundance.³⁷ If one takes the view that the measured ${}^7\text{Li}$ abundance is primordial then the present study puts severe constraints on the physics of the QCD transition as explained. If one remains skeptical of the actual primordial ${}^7\text{Li}$ abundance then it is premature to exclude the study of closed, baryonic universes.

ACKNOWLEDGMENTS

The authors acknowledge useful discussions with J. Audouze, W. A. Fowler, R. A. Malaney, L. McLerran, D. N. Schramm, N. J. Snyderman, G. Steigman, and D. Toussaint. We also acknowledge D. LaPierre for help in the preparation of this manuscript. We would like to acknowledge the Aspen Center for Physics where some of this work was done. This work was performed under the auspices of the U.S. Department of Energy by Lawrence Livermore National Laboratory under Contract No. W-7405-ENG-48.

¹L. G. Yaffe, and B. Svetitsky, Phys. Rev. D **26**, 963 (1982).

²R. D. Pisarski and F. Wilczek, Phys. Rev. D **29**, 338 (1984).

³J. H. Applegate, C. T. Hogan, and R. J. Sherrer, Phys. Rev. D **35**, 1151 (1987).

⁴K. E. Sale and G. J. Mathews, Astrophys. J. **309**, L1 (1986).

⁵C. R. Alcock, G. M. Fuller, and G. J. Mathews, Astrophys. J. **320**, 439 (1987).

⁶E. Witten, Phys. Rev. D **30**, 272 (1984).

⁷J. H. Applegate and C. Hogan, Phys. Rev. D **31**, 3037 (1985).

⁸C. J. Hogan, Phys. Lett. **133B**, 172 (1983).

⁹K. Kajantie and H. Kurki-Suonio, Phys. Rev. D **34**, 1719 (1986).

¹⁰E. V. E. Kovacs, D. K. Sinclair, and J. B. Kogut, Phys. Rev. Lett. **58**, 751 (1987).

¹¹J. Kogut, Phys. Rev. Lett. **56**, 2557 (1986).

¹²M. Fukugita and A. Ukawa, Phys. Rev. Lett. **57**, 503 (1986).

¹³A. H. Guth, Phys. Rev. D **23**, 347 (1981).

¹⁴A. H. Guth and P. J. Steinhardt, Sci. Am. **250**, 116 (1984).

¹⁵See V. Trimble, Annu. Rev. Astron. Astrophys. **25**, 425 (1987).

¹⁶E. Loh and E. Spillar, Astrophys. J. **307**, L1 (1986).

¹⁷R. V. Wagoner, Astrophys. J. **179**, 343 (1973).

¹⁸J. Yang, M. S. Turner, G. Steigman, D. N. Schramm, and K. Olive, Astrophys. J. **281**, 493 (1984).

¹⁹A. M. Boesgaard and G. Steigman, Annu. Rev. Astron. Astrophys. **23**, 319 (1985); G. Steigman (private communication).

²⁰D. Cline (private communication).

²¹D. N. Schramm, in *Electroweak Interactions and Unified Theories*, proceedings of the XXII Rencontre de Moriond, edited by J. Tran Thanh Van (World Scientific, Singapore, 1987).

²²L. D. Landau and E. M. Lifshitz, *Statistical Physics* (Pergamon, New York, 1969).

²³For a discussion of the analytic treatment of relativistic Fermi integrals, see G. M. Fuller, W. A. Fowler, and M. J. Newman, Astrophys. J. **293**, (1985). Previous analytic treatments of quark-gluon plasma in B. Berg *et al.*, Z. Phys. C **31**, 167 (1986); E. Suhonen, Phys. Rev. Lett. **119B**, 81 (1982); K. A. Olive, Nucl. Phys. **B190**, 483 (1981); V. Dixit and E. Suhonen, Z. Phys. C **18**, 355 (1983).

²⁴A. Chodos, R. L. Jaffe, K. Johnson, and C. B. Thorn, Phys.

- Rev. D **10**, 2599 (1974).
- ²⁵A. Chodos and C. B. Thorn, Phys. Rev. D **12**, 2733 (1975).
- ²⁶A. W. Thomas, in *Advances in Nuclear Physics*, edited by J. W. Negele and E. Vogt (Plenum, New York, 1983), Vol. 13, pp. 1–37.
- ²⁷G. E. Brown and M. Rho, Phys. Lett. **82B**, 177 (1979).
- ²⁸S. Théberge, A. W. Thomas, and G. Miller, Phys. Rev. D **22**, 2838 (1980).
- ²⁹L. D. McLerran and B. Svetitsky, Phys. Lett. **98B**, 199 (1981).
- ³⁰Particle Data Group, M. Aguilar-Benitez *et al.*, Phys. Lett. **107B**, 1 (1986).
- ³¹W. A. Fowler and F. Hoyle, Astrophys. J. Suppl. **9**, 201 (1964).
- ³²E. Farhi and R. L. Jaffe, Phys. Rev. D **32**, 2452 (1985).
- ³³C. Alcock and E. Farhi, Phys. Rev. D **32**, 1273 (1985).
- ³⁴M. Crawford and D. N. Schramm, Nature (London) **298**, 538 (1982).
- ³⁵A. Albrecht and N. Turok, Phys. Rev. Lett. **54**, 1868 (1985).
- ³⁶R. Friedberg and T. D. Lee, Phys. Rev. D **15**, 1694 (1977).
- ³⁷P. Delbourgo-Salvador, C. Gry, G. Maline, and J. Audouze, Astron. Astrophys. **150**, 53 (1985); T. Kajino, H. Toki, and S. M. Austin, Astrophys. J. **319**, 531 (1987); J. Audouze and H. Reeves, in *Origin and Distribution of the Elements*, edited by G. J. Mathews (World Scientific, Singapore, in press).
- ³⁸G. J. Mathews and V. E. Viola, Astrophys. J. **228**, 375 (1979).